INTERNATIONAL ATOMIC ENERGY AGENCY
UNITED NATIONS EDUCATIONAL, SCIENTIFIC AND CULTURAL ORGANIZATION
INTERNATIONAL CENTRE FOR THEORETICAL PHYSICS
I.C.T.P., P.O. BOX 586, 34100 TRIESTE, ITALY, CABLE CENTRATOM TRIESTE

SMR. 767 - 4

MINIWORKSHOP ON STRONG CORRELATIONS
AND QUANTUM CRITICAL PHENOMENA
(4 - 22 July 1994)

MOTT TRANSITIONS -
UNIVERSALITY AND VARIETY

Masatoshi IMADA
Institute for Solid State Physics
University of Tokyo
Roppongi 7-22-1, Minato-Ku
Tokyo 106, Japan

These are preliminary lecture notes, intended only for distribution to participants.

MOTT TRANSITIONS

— UNIVERSALITY & VARIETY

M. IMADA

ISSP TOKYO

§1. INTRODUCTION

§2. 2D FERMION CASE

(I) Mass or Density ?

(II) Spin-Charge Separation

(III) Growth of Correlation
— Criticality

§3. General Theory

(I) 1D

(II) 2D Bosons

(III) Classification

(IV) Critical Analysis of Existing Theories

§4. EXPERIMENTAL ASPECTS

(I) Phenomenological Theory of Spin Correlati

(II) Two Types of Mott Transitions
— Charge Crossover and Spin Gap in High-Tc Cuprates

1. Introduction

$\left| \begin{array}{l} \text{gap} \\ \chi = 0 \end{array} \right.$

INCOMPRESSIBLE STATES formed
by many-body interaction

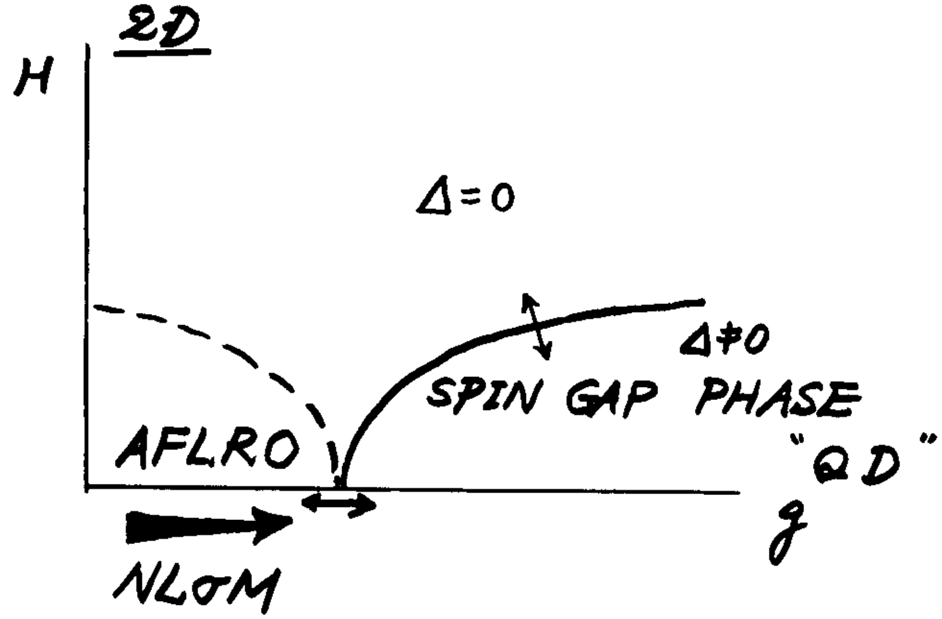

Chakravarty, Halperin & Nelson

Mott insulator charge incompressible

- fermion
- boson

spin gap state spin incompressible

QAFM

1D
- spin integer Haldane
- spin half-integer + dimerization
- spin half-integer + frustration
- even-number chain

2D
- dimerization
- two-layer

FQH state charge incompressible

Quantum Liquid $\longleftrightarrow$ Incompressible States

Transition

- Interest on "critical phenomena" at $T=0$
- Probe for investigating the nature of quantum liquid

.. Realization of <u>anomalous quantum liquid</u>

example

1D Hubbard, Tomonaga-Luttinger liquid

spin-charge separation

χ_c, χ_s . C , D , ...

$\chi_c \neq \chi_s$ at transition

spin, charge correlation

$$\sigma(\omega) = D\,\delta(\omega) + \sigma_{reg}(\omega)$$

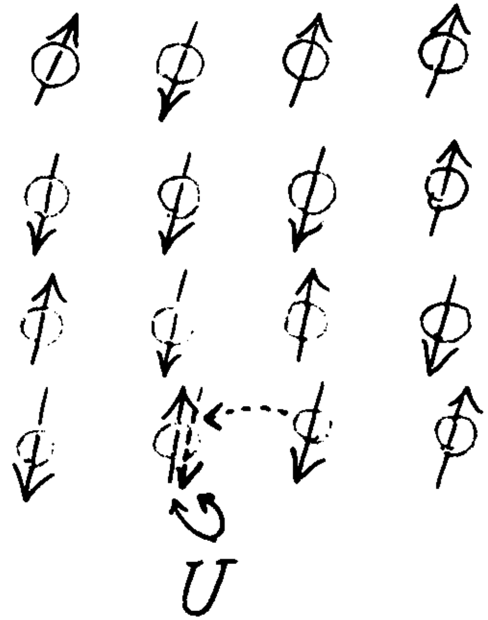

TRANSITION TO MOTT INSULATOR

1937 de Boer Verway NiO
Peierls "strong correlation"
Mott
1949 Mott
Hubbard
70's Brinkman Rice V_2O_3
Hasegawa - Moriya
slave particle
∞ D
QMC

La_2CuO_4
$(La,Sr)_2CuO_4$
$LaTiO_3$
$(La,Sr)TiO_3$
⋮

Mott insulator: ☞ integer number of electrons per unit cell (or site)
☞ band not filled

Mott 1949 NiO

metal $\xrightarrow{\text{Mott transition}}$ Mott insulator (normally A. F.)

A. F. metal

Anderson localization

- typical examples of Mott transition
  $(V,Ti)_2O_3$, $(La,Sr)TiO_3$, cuprates

- Note : two possible routes

  1. change in doping

  2. change in U / t pressure

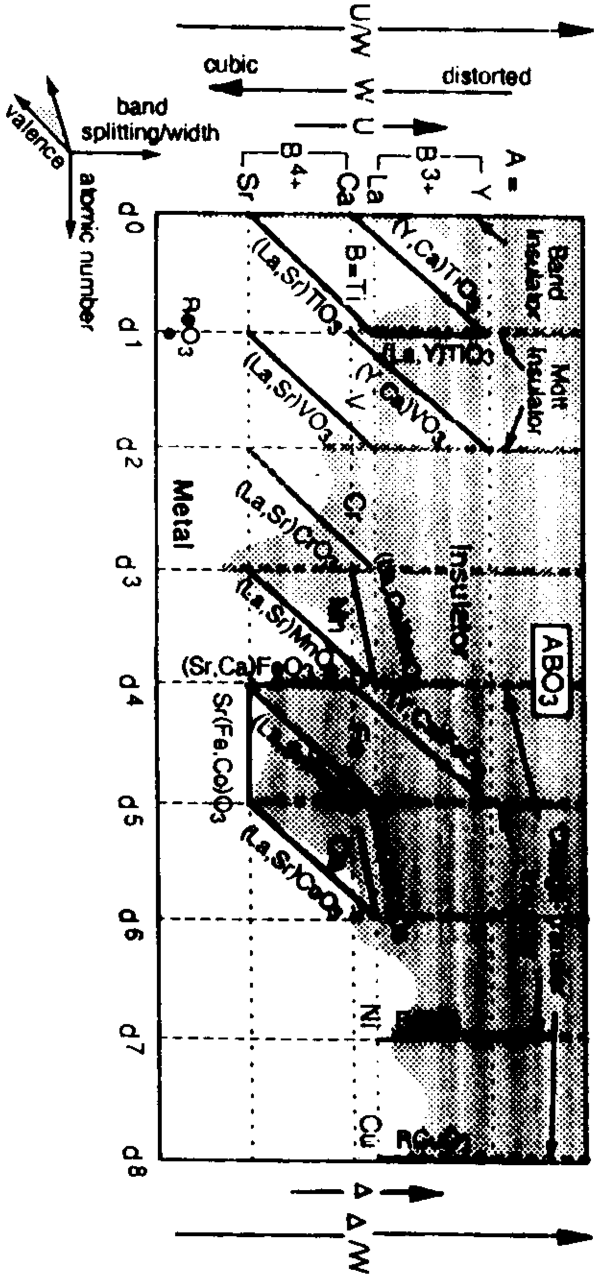

Fig. 1: Various ternary and pseudo-ternary perovskite-type oxides plotted against the A-site cation and the d-band filling n. Band-gap closure occurs along vertical lines; valence control is realized along oblique directions and atomic-number control along the horizontal direction.

§1. INTRODUCTION

RICHNESS OF THE TRANSITION

- route

  U/t

  filling

- magnetic order

	1D	2D	3D	∞D
AF.	×	×	O	O
Ferro	×	×	O	O

3D, ∞D

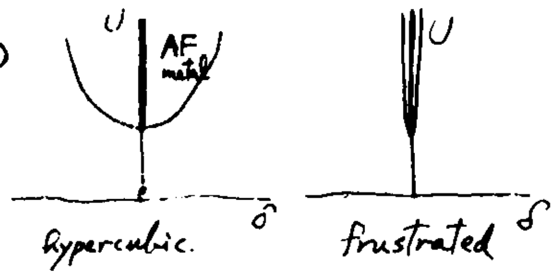

- randomness

  "Mott Anderson Transition."

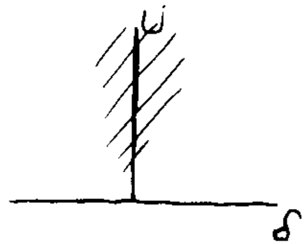

- electron-phonon interaction ↔ Peierls transition cf. DCNQ salt
- phase separation in short-ranged interaction model

Order of the transition

half-filling (change in U/t)

electron-phonon

long-ranged coulomb → (weak) 1st order

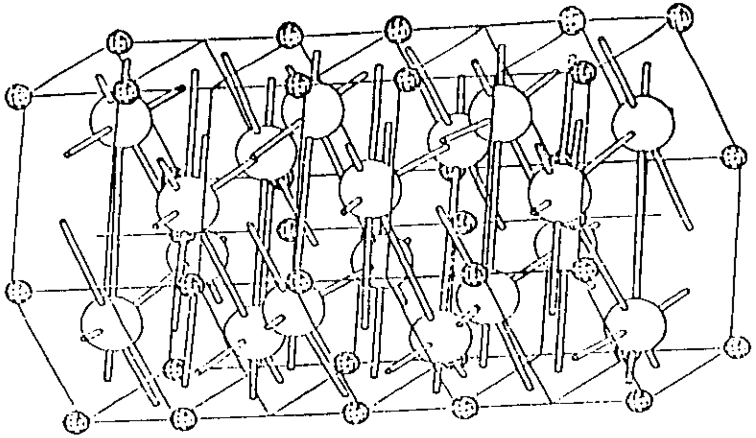

3-73 図 コランダム構造
黒丸：陽イオン, V^{3+},
白丸：陰イオン, O^{2-}

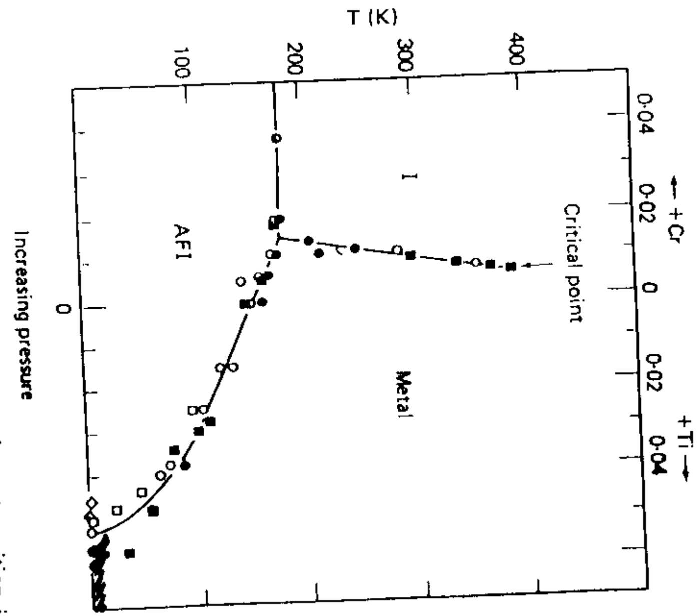

Fig. 6.3 Generalized phase diagram of the metal–insulator transition in V_2O_3 as a function of doping with Cr or Ti and as a function of pressure, showing the critical point (McWhan *et al.* 1971).

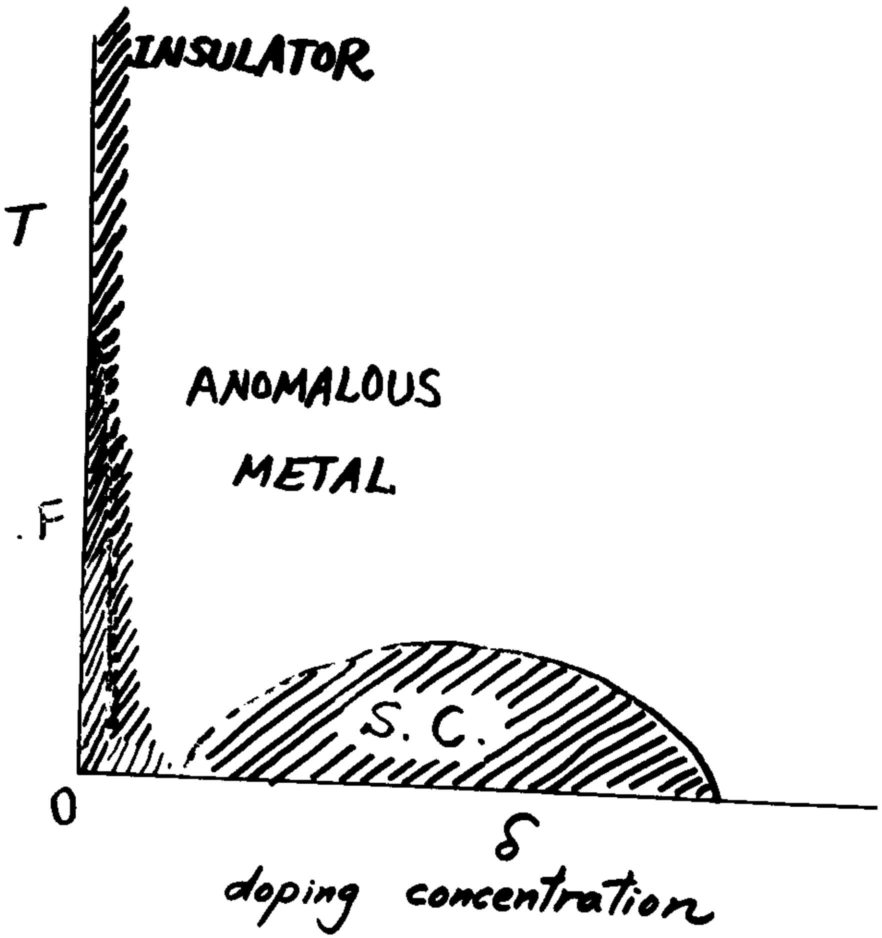

BASIC PHASE DIAGRAM
OF CUPRATES

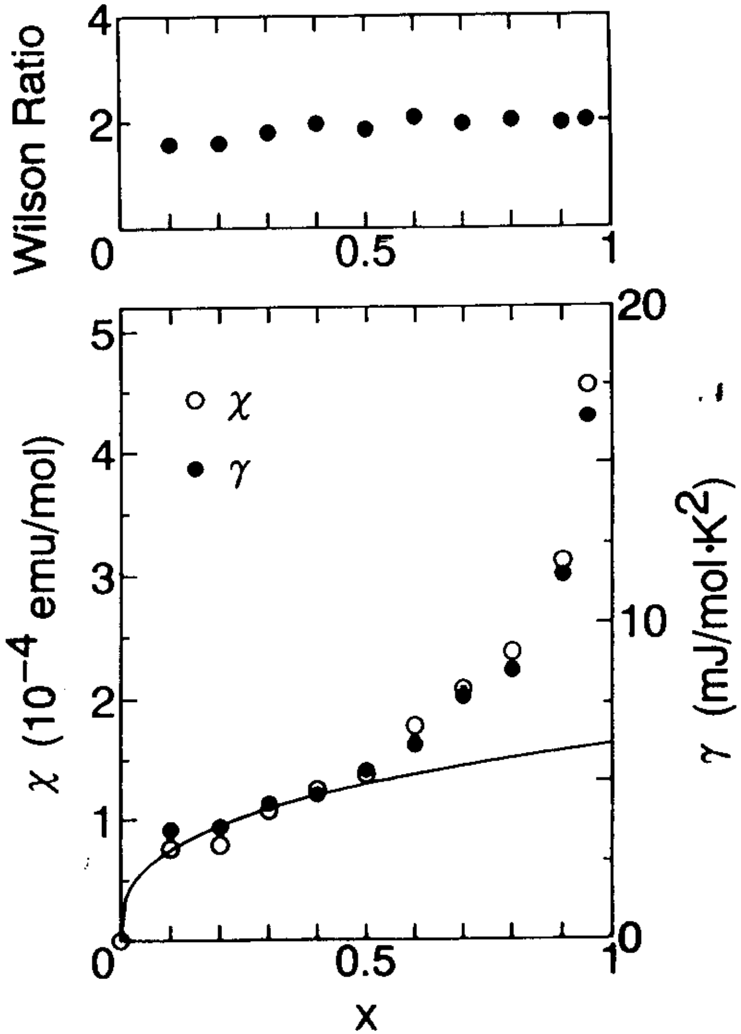

$La_{x} Sr_{1-x} Ti O_3$

Tokura et al.

Fig. 3 Tokura et al.

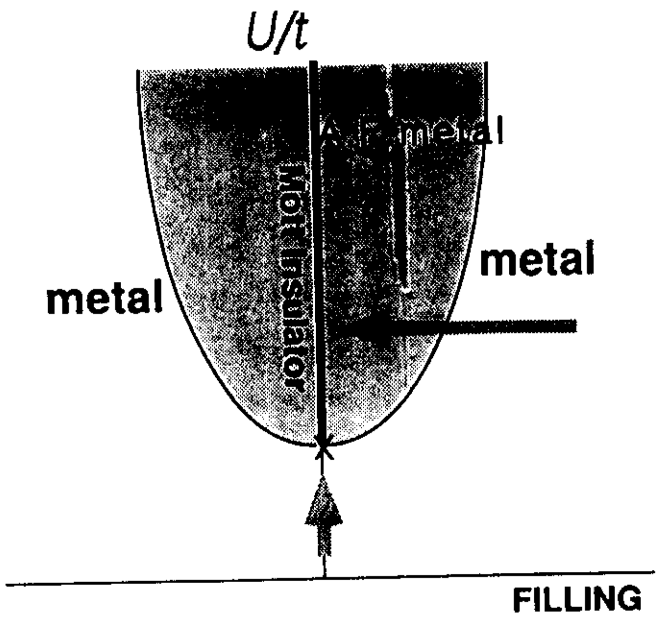

Two Routes to the Mott Insulator

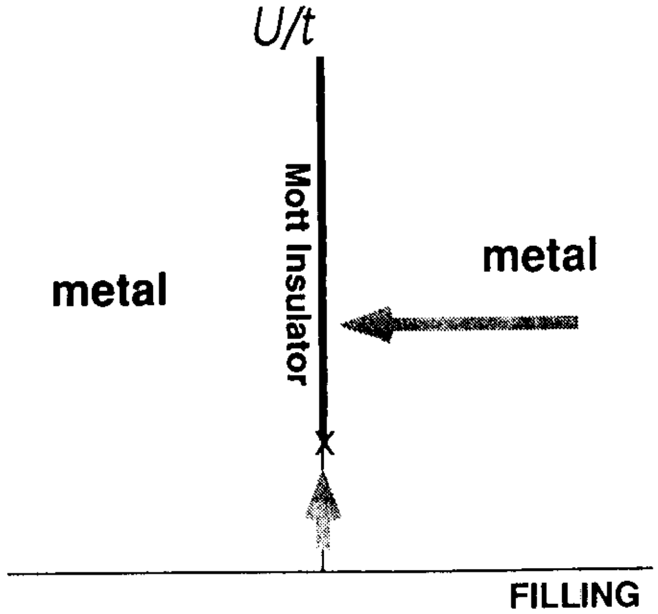

Two Routes to the Mott Insulator

4) A PARADIGM OF THE MOTT TRANSITION

PARAMAGNETIC METAL ⟷ MOTT INSULATOR

SUPPRESSION OF

1) RANDOMNESS ; ANDERSON LOCALIZATION
   - more than or equal to <u>4 components</u> in transition metal oxides
   - careful [illegible] <u>filling control</u>

2) ANTIFERROMAGNETIC METAL
   - <u>low dimensionality</u>
   - careful analysis of lattice structure and orbital degeneracy

3) LATTICE DISTORTION
   structural phase transition

(I)

KINETIC ENERGY IN MOMENTUM SPACE ⟺ SHORT RANGED INTERACTION IN REAL SPACE

COMPETITION

METAL ⟵ ⟶ INSULATOR

- METAL-INSULATOR TRANSITION
- ANOMALOUS METAL

TMO , HTC

bridge → "band structure people"
bridge → "strong correlation people"

-called "Mott insulator"

GROUND STATE OF THE INSULATOR

INERANT PICTURE — Slater

↓

SIC-LDA Svane-Gunnarsson

arametrized HF Grant-McMahan

.DA + U Anisimov - O.K. Andersen

LOCALIZED PICTURE — Mott

↓

CI

⋮

usual circumstances, it is hard to cide superiority between itinerant and calized at $T=0$

ingle particle description is qualitatively lid

DOPING

"BAND PICTURE"

quasi-particle description with Luttinger theorem ⟷ (discontinuously separated) Mott insulator · AF insulator . strongly hybridized insulator

↕

Large fluctuation continuous transition

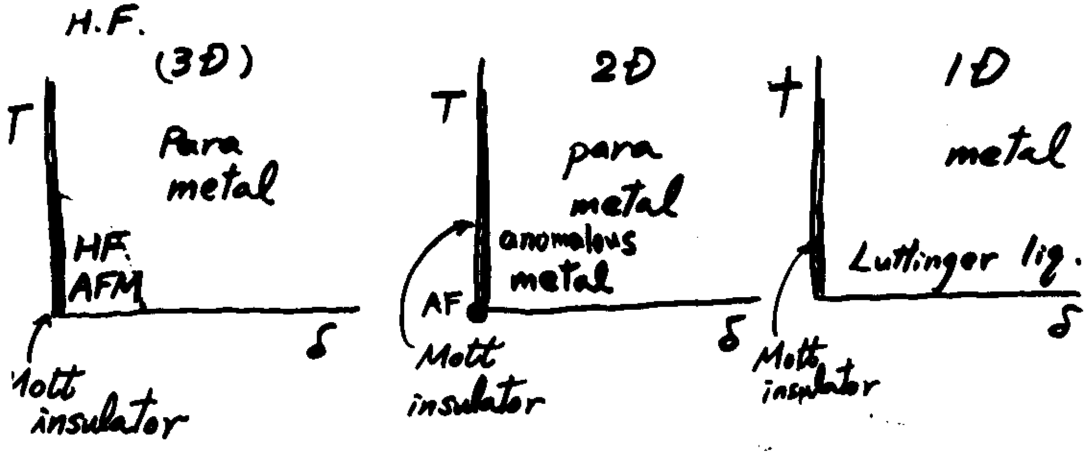

MOTT INSULATOR

SPIN GAP $\Delta_s \neq 0$ { "valence bond insulator"
strong hybridization
↓
low spin state
- $NaCuO_2$
- dimerization
- 2-layer
- 2-chain

$\Delta_s = 0$, no symmetry breaking
- 1D

(AF) symmetry breaking
- La_2CuO_4
- $LaTiO_3$
- ⋮

1) {
- EXCITATION FROM THE INSULATOR
- DOPING → ANOMALOUS METAL

<u>EXCITATION</u>

spin gap ≠ charge gap

↮ "band picture"
Koopman

{ AF insulator → Goldstone mode
"valence bond insulator"
Kondo insulator

ECENT TRENDS

MORE ANOMALOUS STATE!
MORE FLUCTUATION!

0 ⊢——— δ, T ———→

$\boxed{\text{BREAK DOWN}}$ ← "QUASI-PARTICLE"

F
SULATOR → $\boxed{\text{BREAK DOWN}}$

RELEVANT QUANTITIES

Drude weight D

$$\sigma(\omega) = D\,\delta(\omega) + \sigma_{reg}$$

$$D \propto \frac{n}{m^*} \qquad D=0 \text{ at } \delta=0$$

compressibility κ

$$\kappa = \frac{1}{V}\frac{\partial V}{\partial P} = \frac{1}{n^2}\chi_c \qquad \kappa=0 \text{ at } \delta=0$$

incompressible

$$\chi_c = \frac{\partial n}{\partial \mu}$$

density of states $N(\omega)$ $\qquad \Delta_c \neq 0$

uniform susceptibility χ

specific heat coefficient γ

⋮

HOW DOES A METAL BREAK DOWN TO AN INSULATOR ?

||

HOW DOES AN INSULATOR GROW UP FROM A METAL ?

I) MASS or DENSITY ?

$$\sigma(\omega) = D\,\delta(\omega) + \sigma_{reg}$$

$$D \propto \frac{n_c}{m_c^*} \quad \leftarrow \text{ single particle picture}$$

$$\to 0 \left\{ \begin{array}{l} n_c \to 0 \\ m_c^* \to \infty \end{array} \right.$$

M.I. J.P.S.J. 62 (1993) 1105

METAL TO BAND-INSULATOR TRANSITION

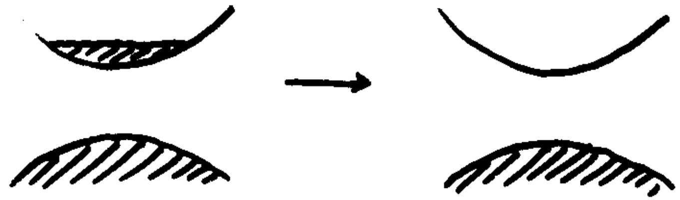

$n \to 0$

$\cancel{m^* \to \infty}$

$\delta \to +0$

$D \to 0$

$$\begin{array}{l} \kappa \\ \chi \\ \gamma \end{array} \to \left\{ \begin{array}{ll} \infty & (1D) \\ \text{const} & (2D) \\ 0 & (3D) \end{array} \right.$$

charge susceptibility
(charge compressibility)

⇒ a direct probe to see the charge mass m_c^*

$T=0$

$$\mu = -\frac{\partial E_g}{\partial n}$$

$$\chi_c = \frac{\partial n}{\partial \mu} \qquad \kappa = -\frac{1}{V}\frac{\partial V}{\partial P} = \frac{1}{n^2}\chi_c$$

cf. isotropic Fermi liquid

$$\chi_c = N(0)\frac{1}{1+F_0^s} \propto m^*$$

$$\chi_s = N(0)\frac{1}{1+F_0^a}$$

$$\chi_c = \frac{1}{N}\int_0^\beta \sum_{ij} n_i(\tau)\, n_j(0)\, d\tau$$

localization ⟷ charge mass

attractive interaction $\begin{cases}\text{phase separation}\\ \text{pairing}\end{cases}$

Metal-Insulator Transition in the Hubbard Model

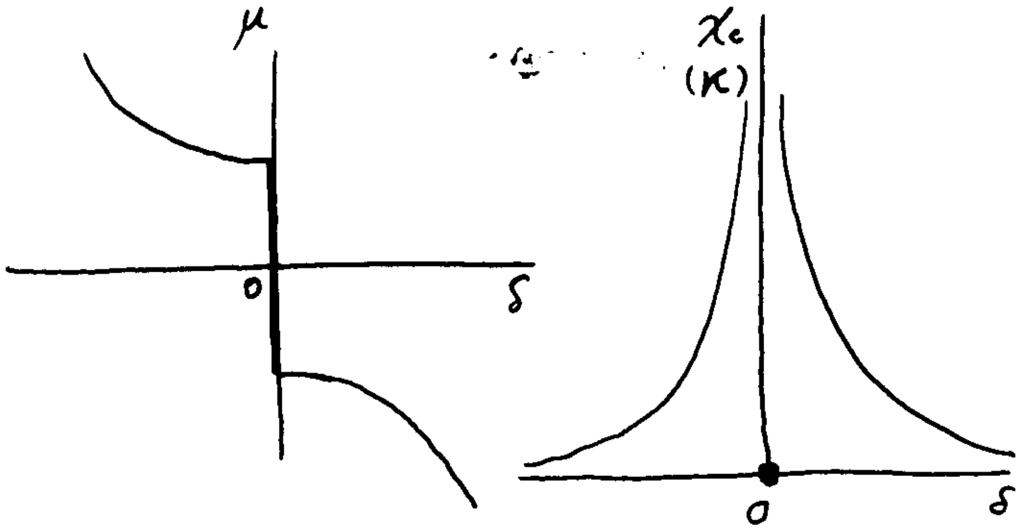

$\chi_c \sim 1/|\delta| \qquad \delta \neq 0$

$\chi_c = 0 \qquad \delta = 0$

→ $m_c^* \to \infty$ as $|\delta| \to 0$

2D Metal-Band Insulator Transition

$m_c^* \to$ finite

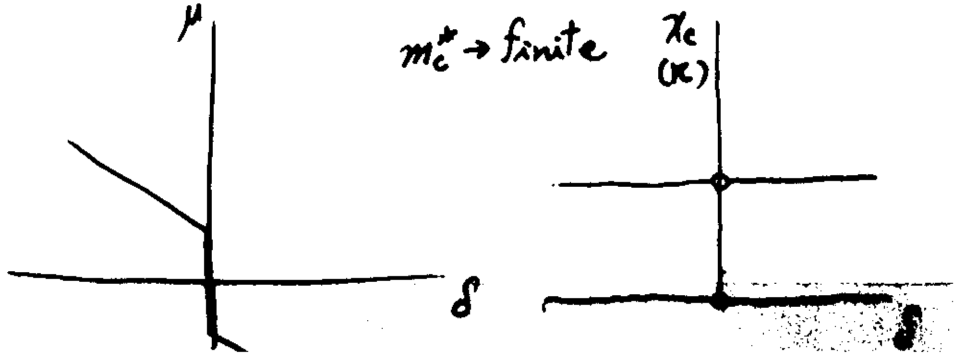

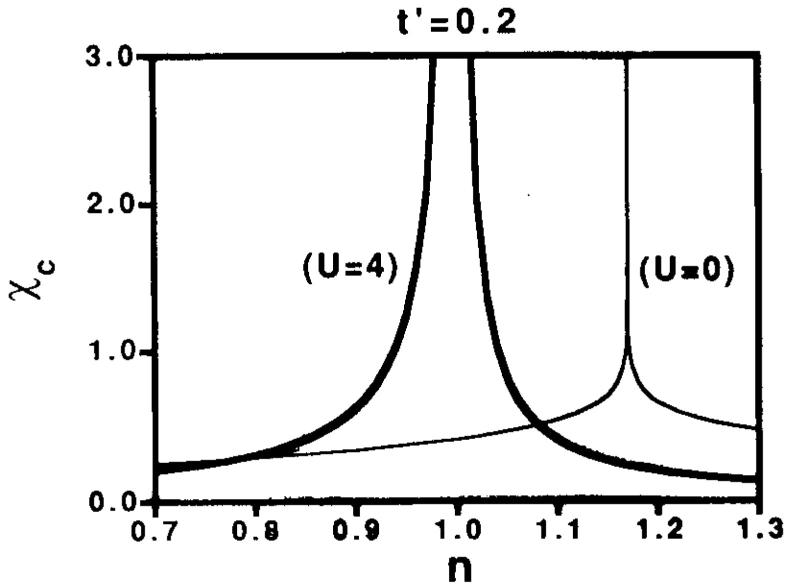

Energy Contour Line of Noninteracting System

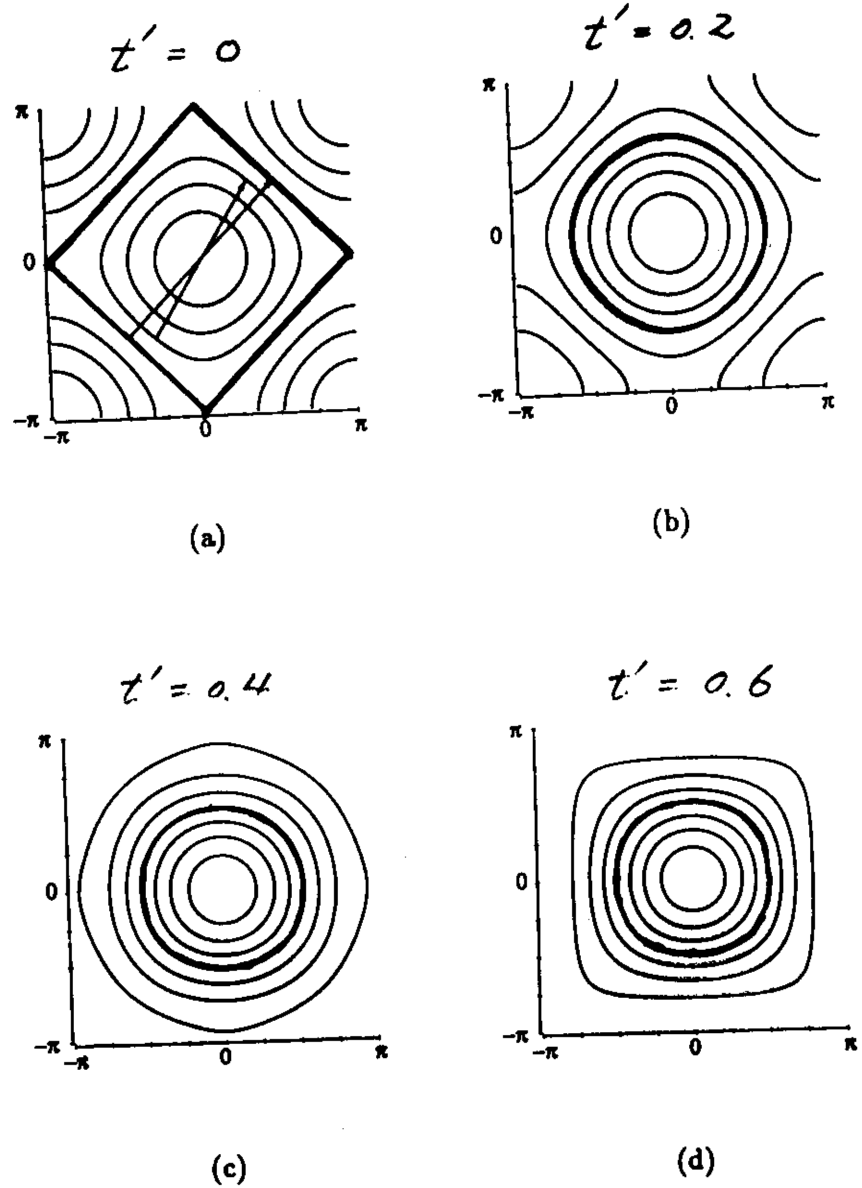

Figure 15

Monte Carlo results of 2D Hubbard

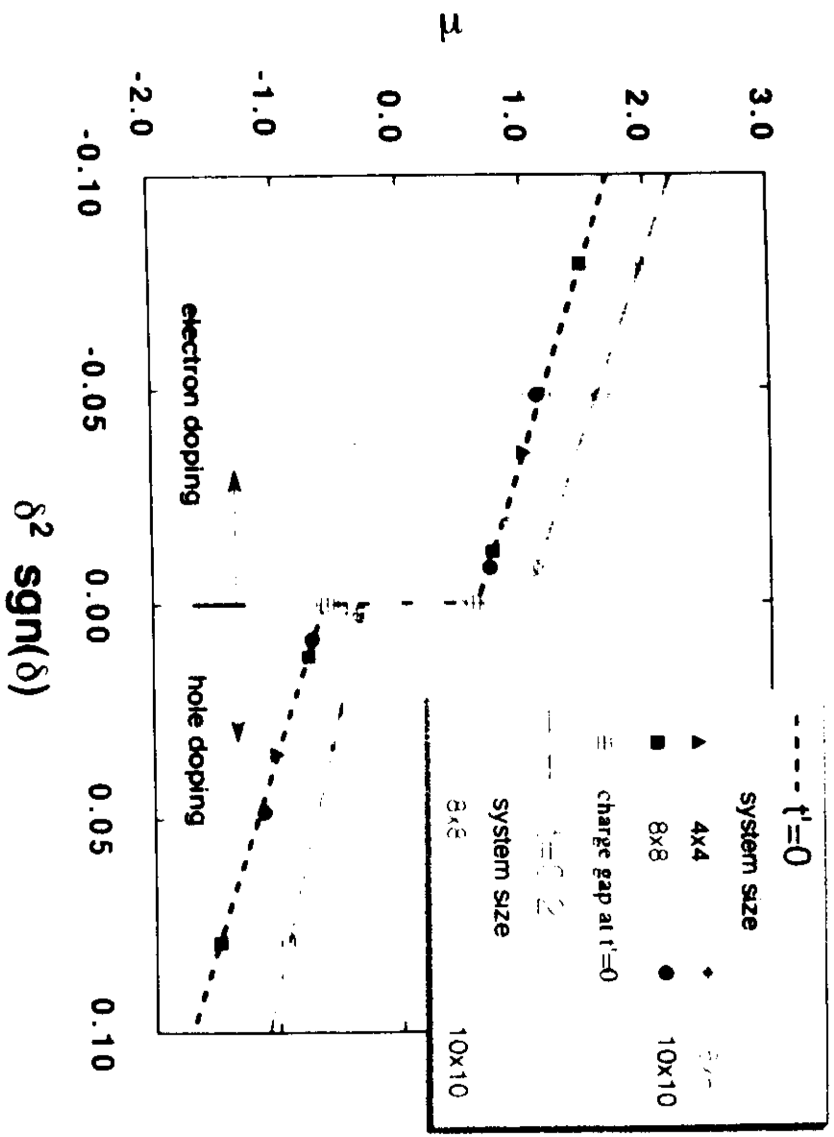

$\mu = \mu_c - a\delta^2$ $\quad \delta = 1 - n$

$\chi_c \propto \delta^{-1}$

charge mass $\quad m_c^* \propto \delta^{-1}$

$t' \neq 0$ $\quad$ ~~electron-hole symmetry~~

~~van-Hove singularity~~ at F.S.

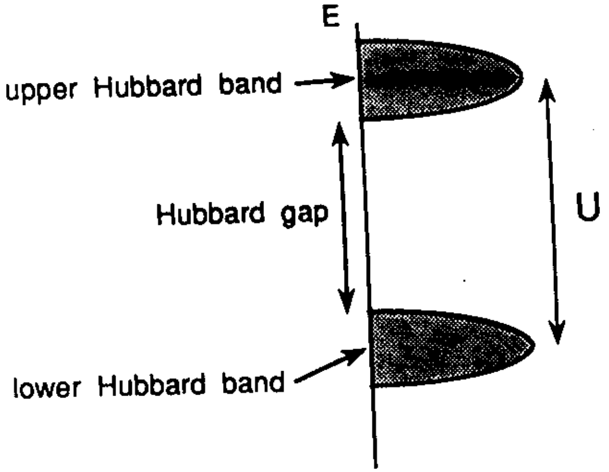

DENSITY OF STATES IN THE HUBBARD APPROXIMATION

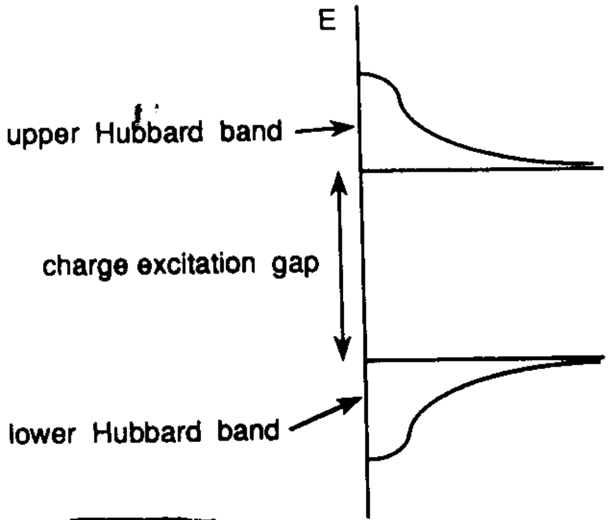

SCHEMATIC CHARGE DENSITY OF STATES OF THE HUBBARD MODEL

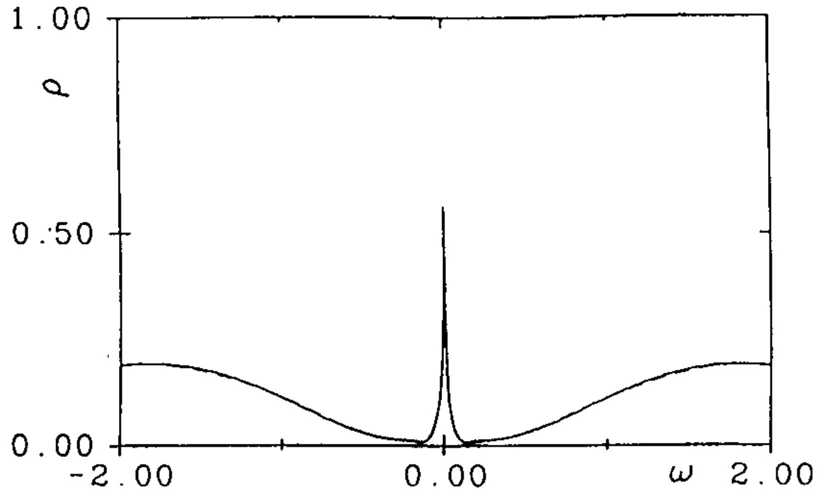

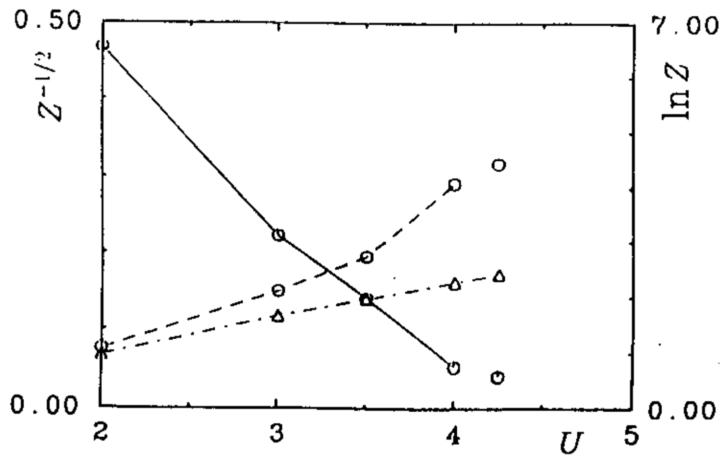

Sakai & Kuramoto

E MECHANISM OF MASS DIVERGENCE IN MULTI-COMPONENT SYSTEMS

IESTED FERMIONS"

HARTREE-FOCK

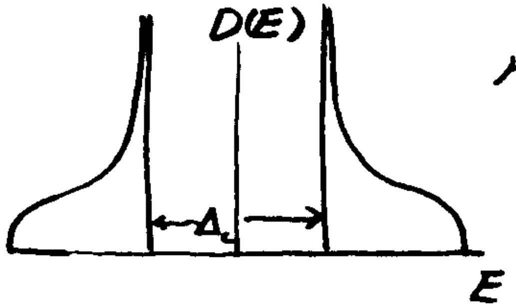

k-independent gap ⟷ square root singularity in D(E)

⇑

destruction of AFLRO immediately upon doping

F ordering as "entropy releasing process"

d law of thermodynamics ↔ cf. ∞D

↕

me kind of ordering in insulator "Kondo resonance"

↓

ass enhancement in metal

THE MECHANISM OF MASS DIVERGENCE

$m_c^* \to \infty$ → is k-dependence $\Sigma(k,\omega)$?

no → κ finite — insulator — para — "Kondo resonance" — ∞D

yes → $\kappa \to \delta^{-1}$ — symmetry breaking (mostly AF) — "GROWTH IN INSULATING (AF) CORRELATION (SPIN)" — 2D

↕ renormalization flow to nesting — cf. H.F.

(II) SPIN-CHARGE SEPARATION

spin gap $\neq$ charge gap

$\not\leftrightarrow$ band picture

spin response $\neq$ charge response

TYPE 1

$$\begin{cases} \chi_c \rightarrow \delta^{-1} \\ \chi_s \rightarrow \text{finite} \end{cases}$$

TYPE 2

metal , superconducting

$$\begin{cases} \chi_c \ \text{finite} \\ \chi_s = 0 \end{cases}$$

$\rightarrow$ 1D

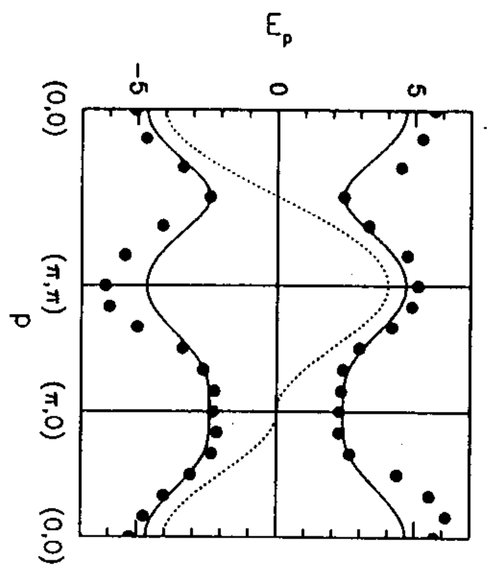

Fig. 4

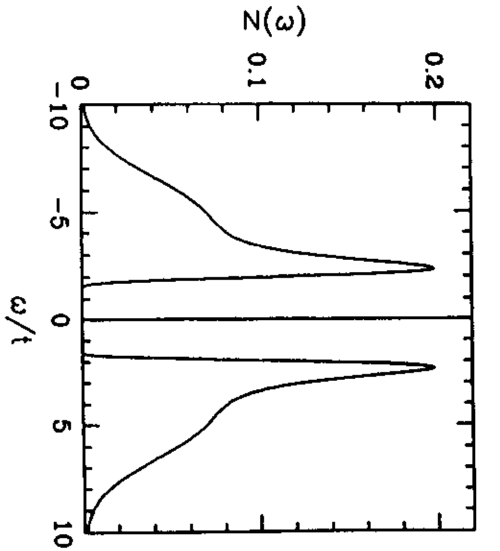

Fig. 3

GENERAL THEORY

1 D case

- fermion Hubbard
- bosons

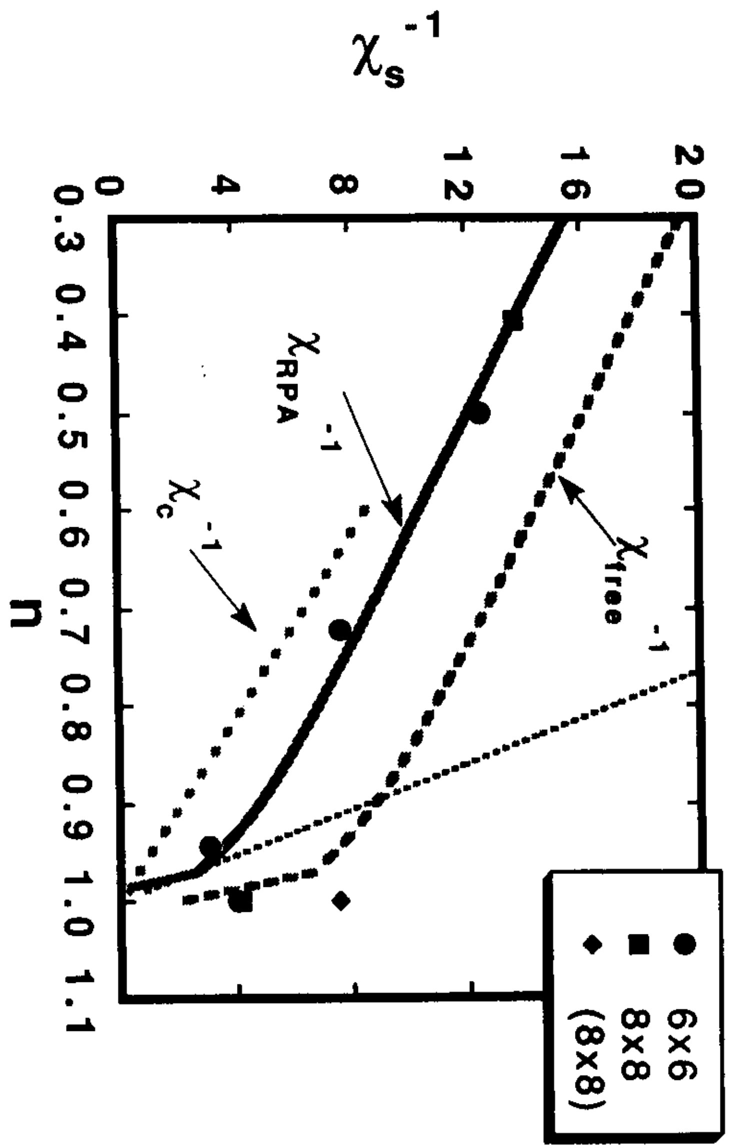

ard-core boson

$$\mathcal{H} = -t \sum_{\langle ij \rangle} (b_i^\dagger b_j + H.c)$$

$$\mathcal{H} = -t \sum_{\substack{\langle ij \rangle \\ s}} (b_{is}^\dagger b_{js} + H.c.) + J_{xy} \sum_{\langle ij \rangle} (S_i^x S_j^x + S_i^y S_j^y) + J_z \sum_{\langle ij \rangle} (S_i^z S_j^z + S_i^z S_j^z)$$

2-component hard-core boson (color / flavor) $J_{xy} = J_z = 0$

boson t-J $J_{xy} = J_z > 0$

modified boson t-J $-J_{xy} = J_z > 0$

boson t-J_z (Ising boson t-J) $J_{xy} = 0$, $J_z > 0$

1D Hubbard

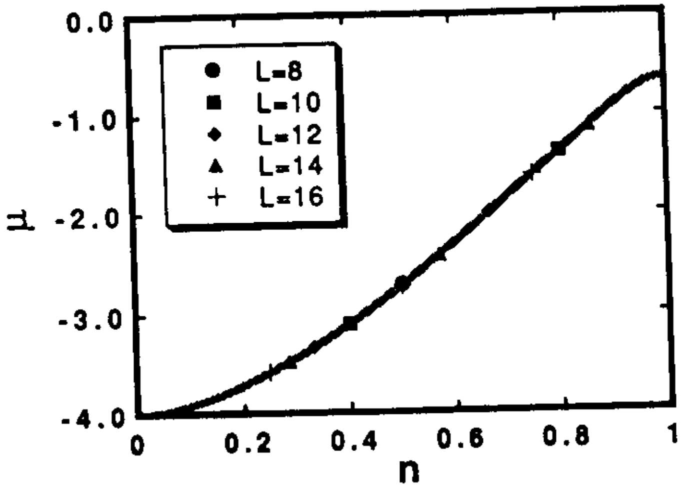

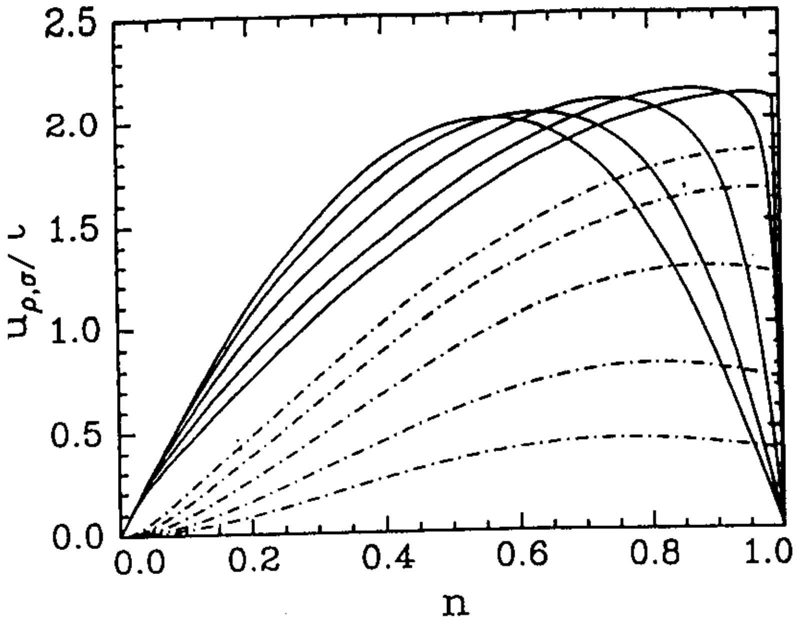

Figure 1: The charge and spin velocities u_ρ (full line) and u_σ (dash–dotted line) for the Hubbard model, as a function of the band filling for different values of U/t: for u_σ $U/t = 1, 2, 4, 8, 16$ from top to bottom, for u_ρ $U/t = 16, 8, 4, 2, 1$ from top to bottom in the left part of the figure.

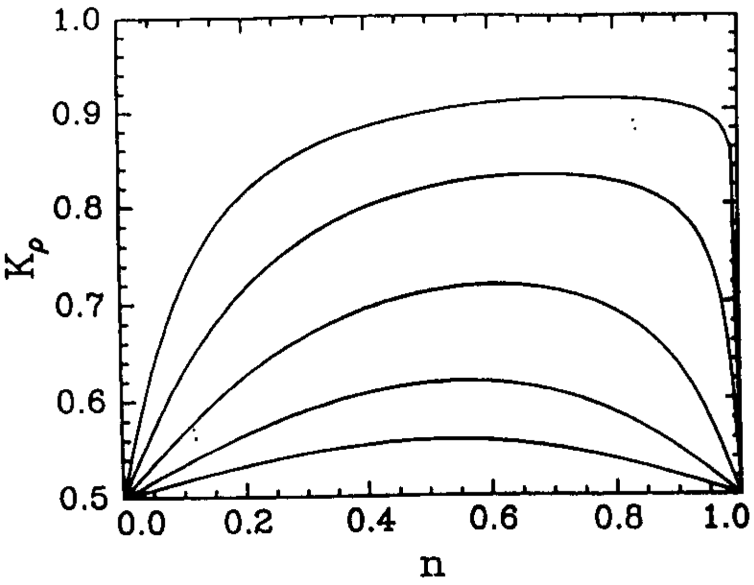

Figure 3: The correlation exponent K_ρ as a function of the bandfilling n for different values of U ($U/t = 1, 2, 4, 8, 16$ for the top to bottom curves). Note the rapid variation

	χ_c	γ	χ_s
fermion Hubbard	δ^{-1}	δ^{-1}	const
$t-J$			

$\delta \to 0$ $\quad$ $v_c \to 0$

$v_s \to$ finite

hard core boson

$$\mathcal{H} = -t \sum_{\langle ij \rangle} b_i^\dagger b_j$$

$\longleftrightarrow$ XY model

Katsura $\quad m = \frac{1}{\pi} \sin^{-1}\left(\frac{H}{J}\right)$

$$\begin{cases} S^z = 1/2 \to n = 1 \\ S^z = -1/2 \to n = 0 \end{cases} \quad J S_i^+ S_j^- \to t c_i^\dagger c_j$$

$$\chi_c = \frac{2}{\pi} \frac{1}{\sqrt{t^2 - \mu^2}}$$

$$\chi_c \propto \delta^{-1}$$

$$\gamma \propto \delta^{-1}$$

hard core boson $\quad C \propto T \leftarrow \varepsilon \propto q$

free boson $\quad C \propto T^{1/2} \leftarrow \varepsilon \propto q^2$

mapping between $\delta \leftrightarrow 1 - \delta$

1D

All the Mott transitions have the same feature

$$\begin{cases} \chi_c \propto \delta^{-1} \\ \gamma \propto \delta^{-1} \\ \chi_s \sim \text{const.} \end{cases}$$

⊙ Mott transition $\longleftrightarrow$ · band insulator transition

$\chi_c \propto \delta^{-1}$
$\gamma \propto \delta^{-1}$ · interacting bosons $n \to 0$

⊙ "spin-charge separation"

$\chi_c \leftrightarrow \chi_s$

fermion Hubbard.
t-J
hard-core boson
"two-color" hard-core boson
boson t-J

§2.2 2D

	χ_c	γ	χ_s
fermion Hubbard	δ^{-1}	(δ^{-1})	const

$m_c^* \propto \delta^{-1}$

hard core boson

$\chi_c \sim$ const. (log) $\quad C \propto \gamma T^2 \leftarrow \varepsilon \propto q$

p. h. transformation $\quad C \propto T$ at $n=1$ $\leftarrow \varepsilon \propto q^2$

$\delta \longleftrightarrow 1-\delta$

$n \to 0$ c.f. spinless fermion

"two (color) flavor" hard core boson

the same as "one flavor" boson

same ground state distinguishable $\updownarrow$ boson

boson t-J

- "antiferromagnetic" order at $n=1$
- $\chi_c \to \infty$
- $\chi_s \sim$ finite

"flavor"-charge separation

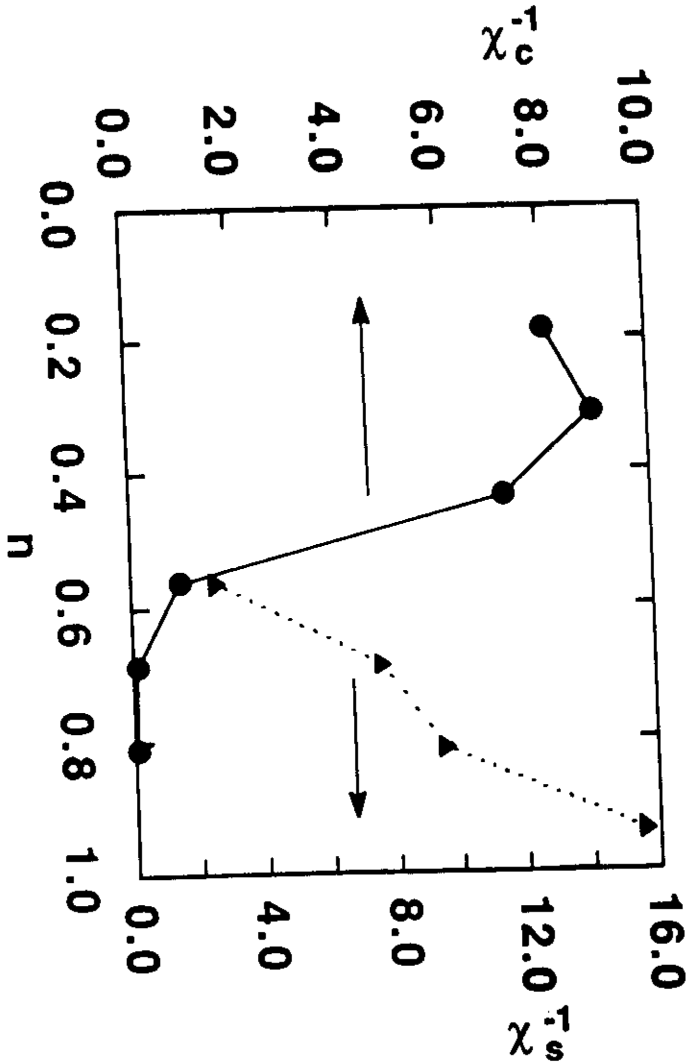

χc-1
0.0
2.0
4.0
6.0
8.0
10.0
0.0
0.2
0.4
0.6
0.8
1.0
n
0.0
4.0
8.0
12.0
16.0
χs-1

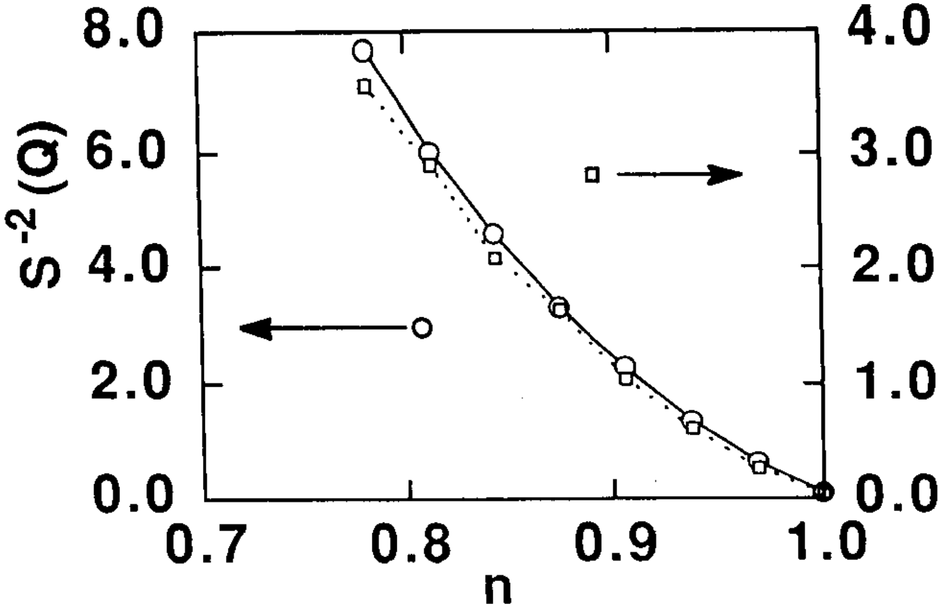

8.0
6.0
4.0
2.0
0.0
S-2(Q)
4.0
3.0
2.0
1.0
0.0
χ-1(Q)
0.7
0.8
0.9
1.0
n

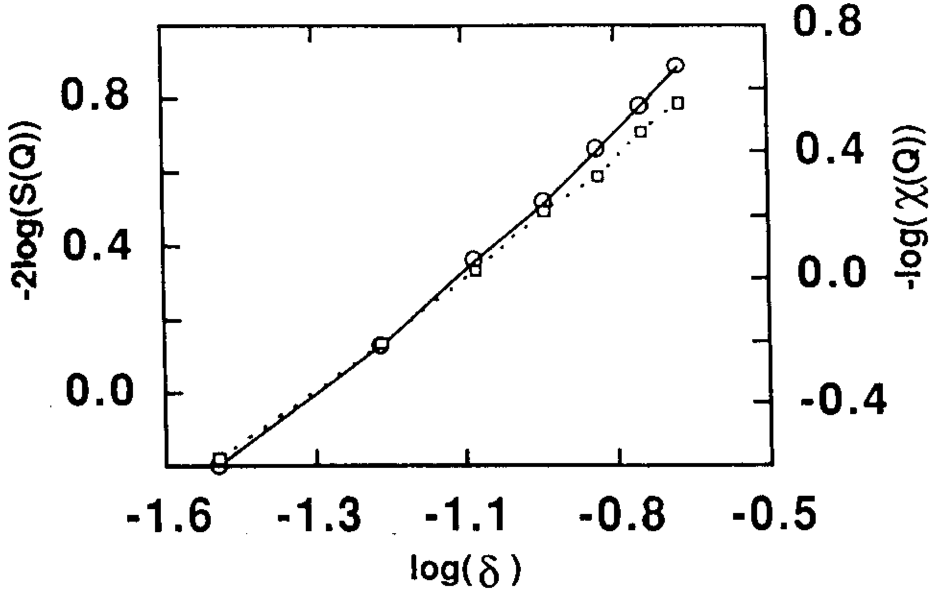

0.8
0.4
0.0
-2log(S(Q))
0.8
0.4
0.0
-0.4
-log(χ(Q))
-1.6
-1.3
-1.1
-0.8
-0.5
log(δ)

Fig. 5 2

M. IMA

-2log(S(Q))

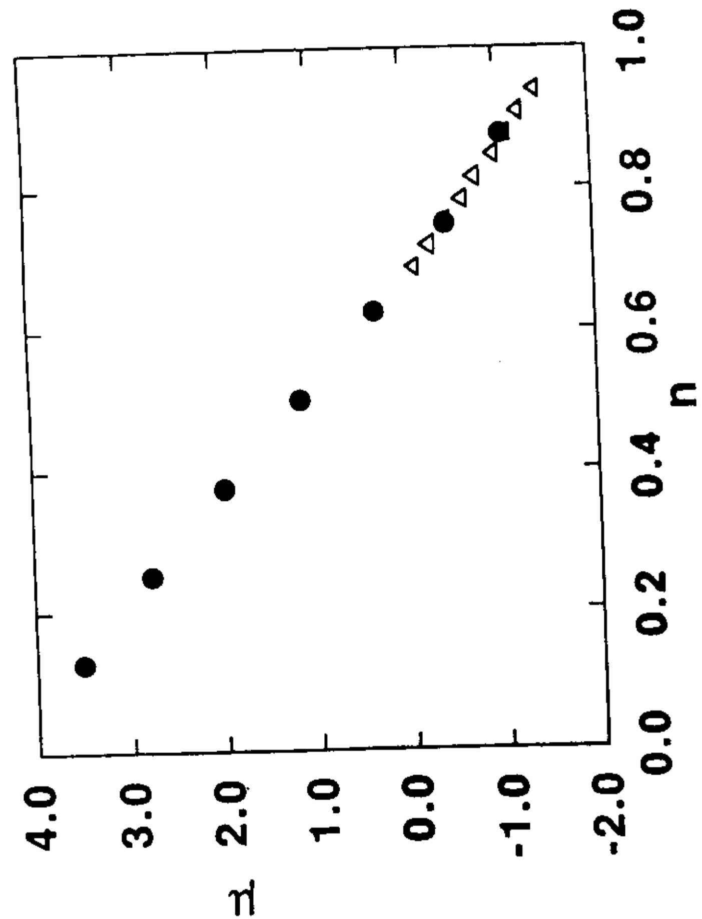

Fig. 6

M. Imada

General theory of Mott transitions

- statistics
- # components
- dimensionality
- interaction

at least useful classification

$$\begin{cases} m_c^* \to \infty \\ n_c \to 0 \end{cases}$$

1D universal. χ_c γ D
χ_s

2D variety

fermion → multi-component → $m_c^* \to \infty$.

boson → single-component → $n \to 0$

boson → multi-component → $n \to 0$

multi-component → interaction → $m_c^* \to \infty$

Mott insulator		M-I transition	metal: electronic system	metal: more generally
<u>spin gapless</u> AF insulator		TYPE 1 $m_c^* \to \infty$	spin gapless metal eg. fermi liquid tomonaga-Luttinger liq.	multi-component quantum fluid
High T_c?	BAND PICTURE			
<u>spin gap</u> "valence bond insulator" strongly hybridized insulator		TYPE 2 $n_c \to 0$	spin gap metal $\Rightarrow$ super cond. at $T=0$	1-component quantum fluid superconductivity or superfluid

CHARGE COMPRESSIBILITY

$$\kappa = \frac{1}{V}\frac{\partial V}{\partial P} = \frac{1}{n^2}\chi_c$$

$$\chi_c = \frac{\partial n}{\partial \mu}$$

$\kappa = 0$ at $\delta = 0$: insulator

incompressible

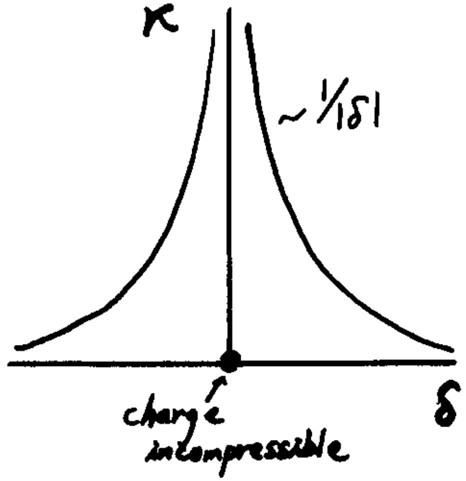

TYPE 1

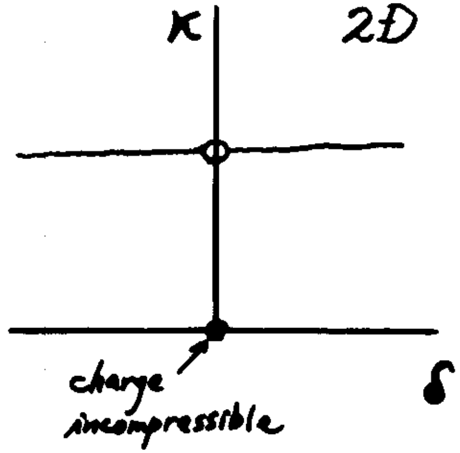

TYPE 2

if $\kappa \to \delta^{-1} \Rightarrow m_c^* \to \infty$

	κ	χ_s	γ	z	δ_c	"fermi surface"	D(E)	A.F.
ubbard III	const (2D) δ (3D)	const (2D) δ (3D)	const(2D) δ (3D)	1	0	small		×
utzwiller	const (2D) δ (3D)	δ^{-1}	δ^{-1}	δ	0	large		×
IF-RPA	const	const	const	const ~ 1	large (metallic AF)	large small	ε^{-1} $\ln\varepsilon$	○
0D para	(δ)	$\sim 1/J$	δ^{-1}	δ	0	large		×
lave-boson -gauge-field (2D)	const (log)	const	const	/	?			?
D Hubbard M.C.	δ^{-1}	const $\sim J^{-1}$	(δ^{-1})	/	~ 0	large	ε^{-1}	○

III) GROWTH OF CORRELATION LENGTH

— CRITICALITY —

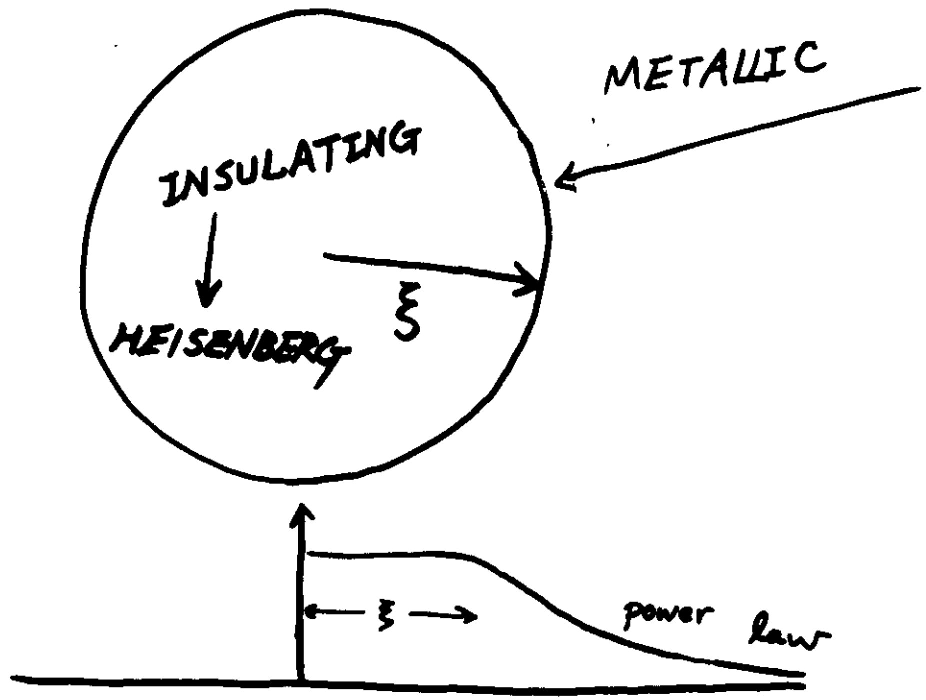

transition is always driven by the shorter length scale ξ

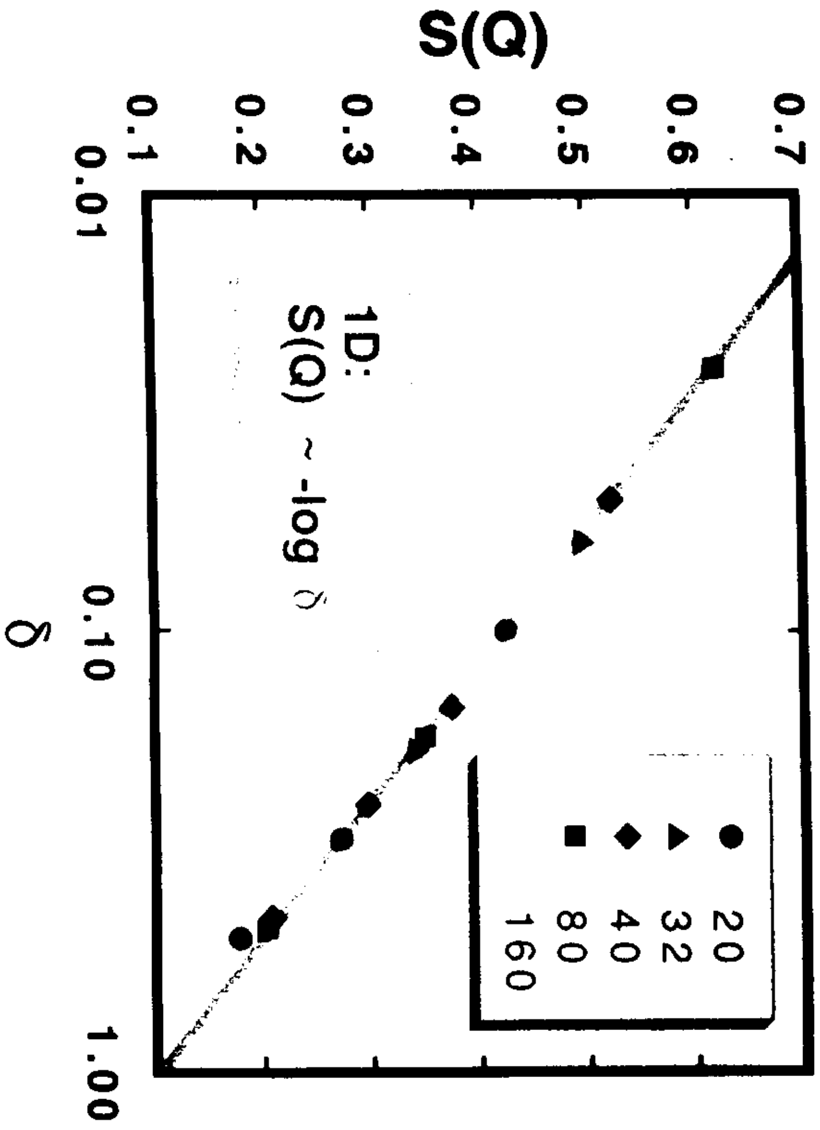

§3. Antiferromagnetic Transition

§3.1. 1D Hubbard model

$$S(Q) = \int dr \langle S(0)\cdot S(r)\rangle e^{-iQr}$$

Q: incommensurate wave vector

$$Q = \pi(1-\delta)$$

$$S(Q) \propto -\ln \delta$$

$$\langle S(0)\cdot S(r)\rangle \propto \begin{cases} \frac{1}{r} e^{-iQr} & r<\xi \\ \frac{1}{r^{\gamma}} e^{-iQr} & r>\xi \end{cases}$$

$$\xi = \delta^{-1}$$

crossover length

$U=\infty$ Hubbard $f = Z\Phi$

$$\langle S(0)\cdot S(r)\rangle \propto \frac{1}{r}\exp\left[-\frac{1}{2}\{\ln(\delta r) - ci(2\pi\delta r) - \cos(2\pi\delta r) - 2\pi\delta r\, si(2\pi\delta r)\}\right]$$

$$\sim \begin{cases} e^{-iQr}/\delta^{1/2} r^{3/2} & \delta r \gg 1 \\ e^{-iQr} e^{-\pi^2\delta r/2}/r & \delta r \ll 1,\ r \gg 1 \end{cases}$$

$Q = \pi(1-\delta)$ $\xi = \delta^{-1}$

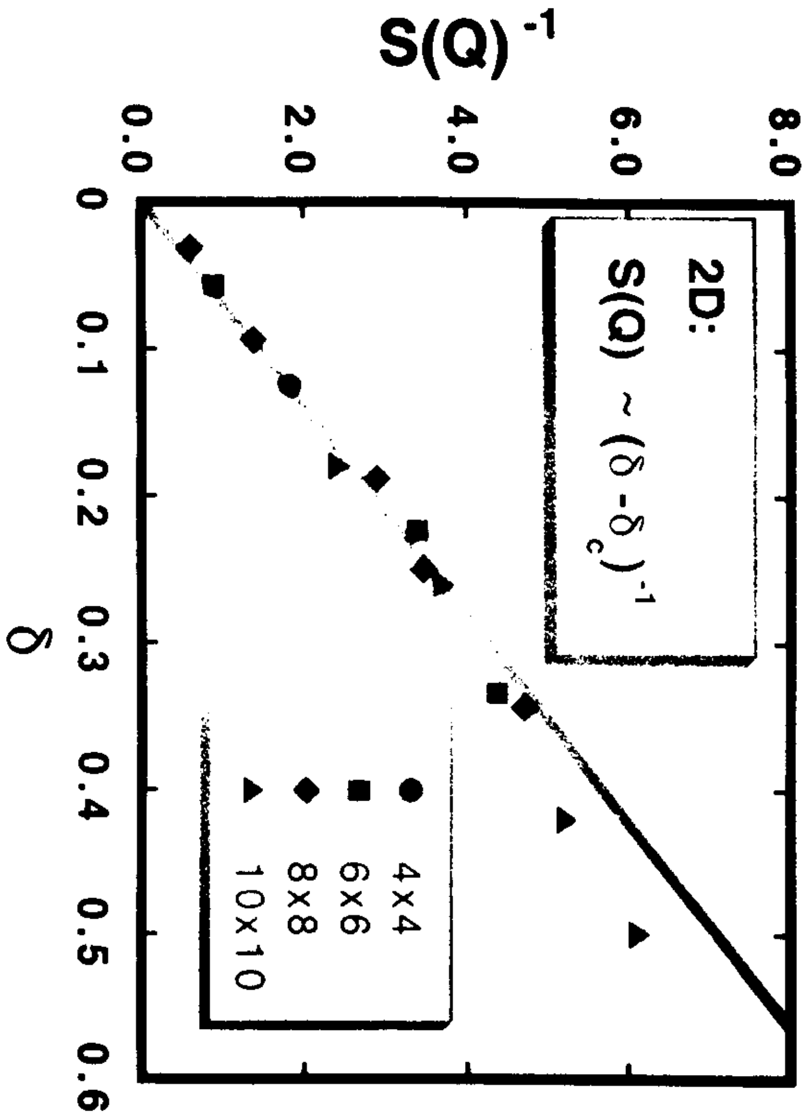

A. F. ordering of 2D & 1D Fermions

different from the usual critical phenome[na]

2D

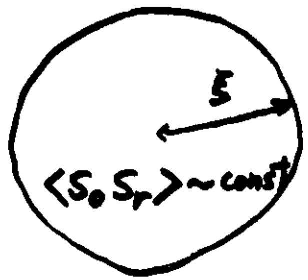

$\langle S_0 S_r \rangle \sim \frac{1}{r^\gamma}$

$2 < \gamma \le 3$

$S(Q) \propto \delta^{-1}$ "$\nu = 0.25$"

1D

$\langle S_0 S_r \rangle \sim \frac{1}{r}$ ξ $\langle S_0 S_r \rangle \sim \frac{1}{r^\gamma}$ $1 < \gamma \le 2$

$S(Q) \propto \ln \delta$

$\xi \to \infty$ as $\xi \propto \delta^{-1/d}$

$\Big\{$ ξ well defined
power law asymptotically

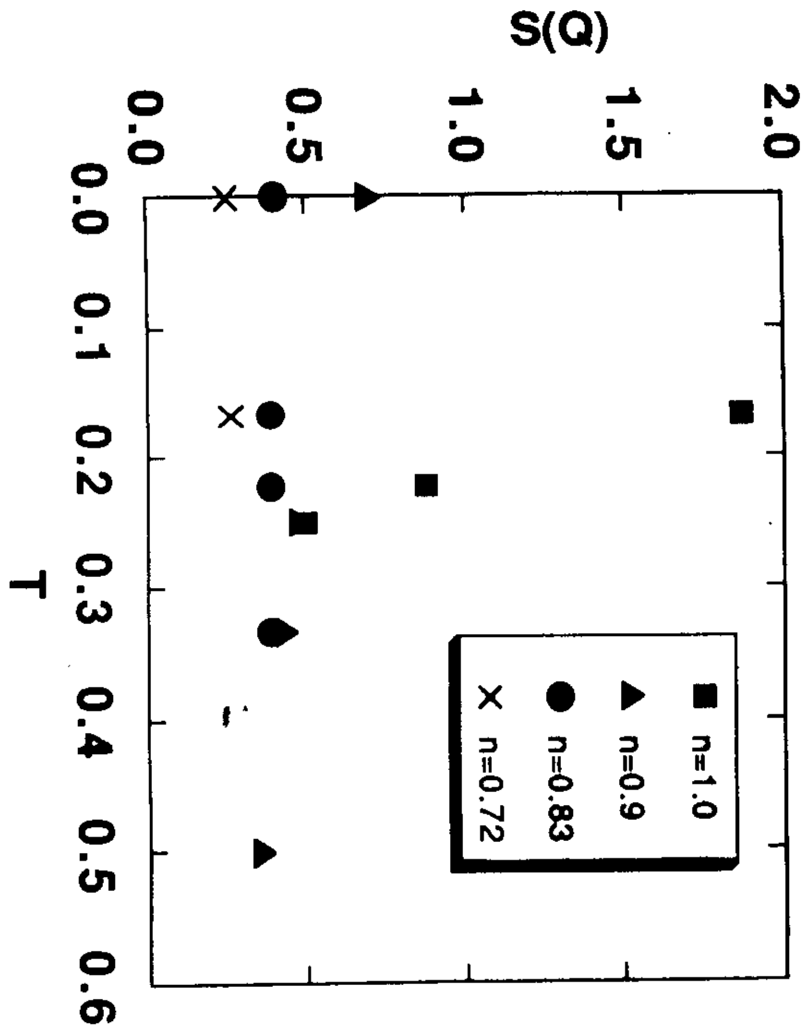

M.C. Results on A.F. Correlation

① $T=0$

$$\int S(Q,\omega)\,d\omega \propto \delta^{-1}$$

$$\updownarrow$$

$$\xi_0 \simeq a\,\delta^{-1/2}$$

② $r > \xi_0$ metallic CROSSOVER

$r < \xi_0$ insulating

③ $\int S(Q,\omega)\,d\omega$, ξ

weak T-dependence at low T

④ no evidence for spin gap in canonical models

(31+31)/8x8

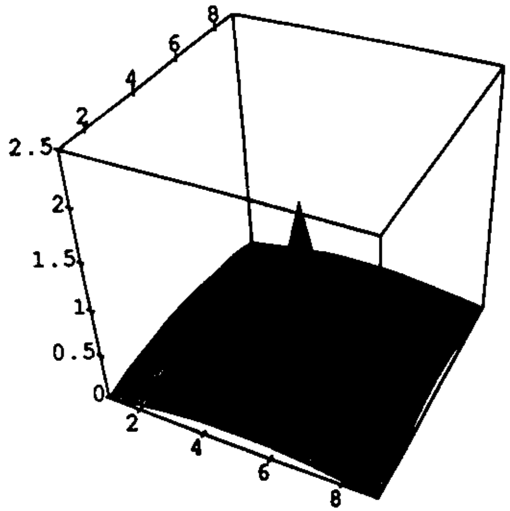

(32+32)/8x8

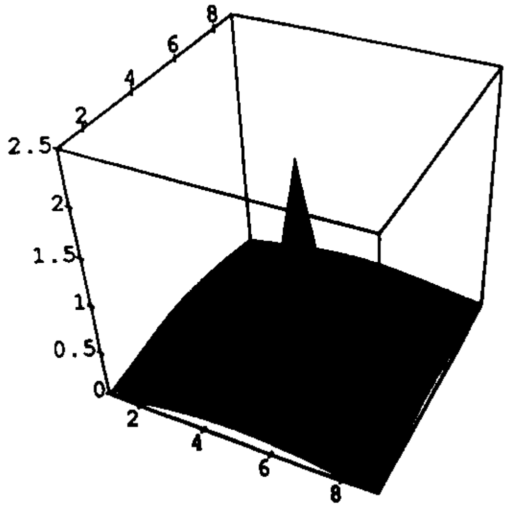

$\frac{82}{10 \times 10}$

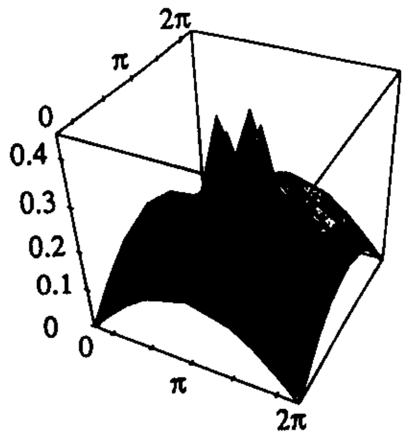

$\frac{74}{10 \times 10}$

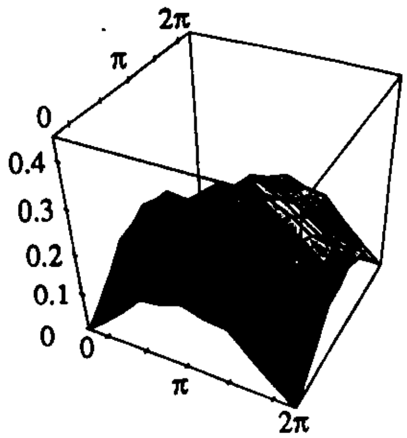

$\frac{58}{10 \times 10}$

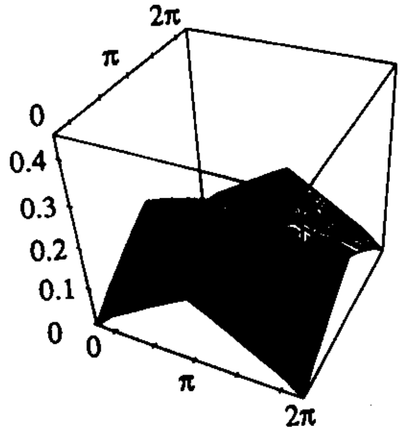

$\frac{50}{10 \times 10}$

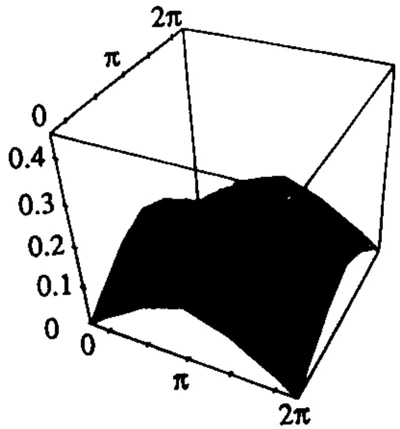

RPA does not reproduce the correct
-itical behavior

$$\chi_{RPA} = \frac{\chi_0}{1 - U\chi_0}$$

$$Im\,\chi_{RPA} = \frac{Im\,\chi_0}{(1 - U\,Re\,\chi_0)^2 + (U\,Im\,\chi_0)^2}$$

$$= \frac{c\omega + \cdots}{a(\delta - \delta_c)^2 + b\omega^2 + \cdots}$$

$$S(Q,\omega) = \frac{1}{1 - e^{-\beta\omega}}\;\frac{c\omega + \cdots}{a(\delta - \delta_c)^2 + b\omega^2 + \cdots}$$

$T = 0$

$$S(Q, t=0) = \int_{-\infty}^{\infty} S(Q,\omega)\,d\omega \simeq \frac{c}{2b}\ln\frac{b}{a(\delta - \delta_c)^2}$$

$$S(Q, t=0) \sim \ln(\delta - \delta_c)$$

cf. t-J $\quad U \to J_{Q}$

T_{scr1}

CROSSOVER OF ξ

ξ_0 : <u>intrinsic correlation length</u> at $T=0$

$$\xi_0 \simeq a\,\delta^{-1/2}$$

$r < \xi_0$: Heisenberg-like $\quad \langle S(0)S(r)\rangle \sim e^{iQr} \times \text{const.}$

$r > \xi_0$: metallic $\quad \langle S(0)S(r)\rangle \sim e^{iQr} \cdot r^{-\eta}$

$\eta > 2$

ξ_T : <u>thermal correlation length</u>

$$r < \xi_T : \quad \langle S(0)S(r)\rangle \begin{cases} \sim e^{iQr}\cdot \text{const} \\ \sim r^{-\eta}\cdot e^{iQr} \end{cases}$$

$$r > \xi_T : \quad \langle S(0)S(r)\rangle \sim e^{-r/\xi_T}$$

$\xi_T \to \infty \quad$ as $\quad T \to 0$

ξ : $\quad Min(\xi_0, \xi_T)$

<u>effective correlation length</u>

$$r < \xi : \langle S(0)S(r)\rangle \sim e^{iQr}$$

$$r > \xi : \langle S(0)S(r)\rangle \sim \begin{cases} e^{-r/\xi} \\ r^{-\eta} \qquad \eta > 2 \end{cases}$$

C-H-N

Makivić - Ding $\quad \xi_T \sim b\, \exp[cJ/T]$

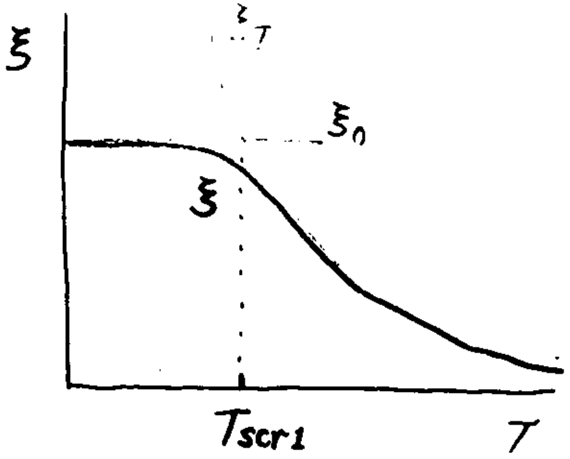

$$T_{scr1} \simeq -2cJ \frac{1}{\ln\left[\left(\frac{a}{b}\right)^2 \delta\right]}$$

$J \sim 1500\,K$

$a/b \sim 0.4$

$c \sim 1.2$

$f(q, \omega, \kappa)$: metallic regime

$\frac{f(q,\omega,\kappa)}{\omega}$
- peak at $q = \omega = 0$ ← short-ranged A.F. correlation
- T-independent

c.f. RPA

$$f(q, \omega, \kappa) = \frac{\tilde{C}\,\omega}{\tilde{D}^2(\kappa^2+q^2)^2+\omega^2}$$

$\tilde{C}$, $\tilde{D}$, κ : T-independent

- incommensurability
- $2k_F$ singularity

disordered insulating regime

hydrodynamic approach $\quad$ Kawasaki

mode-mode coupling

$$\int dr\, e^{iqr} \langle S(r,t)\, S(0,0) \rangle \propto e^{-t/\tau(q)}$$

T_{scr2}

CROSSOVER BETWEEN METALLIC AND INSULATING

for $\omega > 0$

$$\mathrm{Im}\,\chi(q,\omega) \sim \begin{cases} f(q,\omega,\kappa) & \mathrm{Max}(T,\omega) < T_{scr2} \\ \dfrac{C(1-e^{-\beta\omega})}{\omega^2 + D^2(\kappa^2+q^2)^2} & \mathrm{Max}(T,\omega) > T_{scr2} \end{cases}$$

disordered hydrodynamic region

$\kappa \equiv \xi^{-1}$

$T_{scr2} \sim \tau^{-1} \equiv D(\kappa^2 + q^2)$

for $\omega < 0$ $\leftarrow$ $\mathrm{Im}\,\chi(q,-\omega) = -\mathrm{Im}\,\chi(q,\omega)$

$q \equiv k - Q$ hydrodynamic region

$\mathrm{Max}(T,\omega) < T_{scr2}$: metallic

$\mathrm{Max}(T,\omega) > T_{scr2}$: insulating

κ : always T-independent

$\uparrow$

$\because T_{scr2} < T_{scr1}$

EXPERIMENTAL INDICATIONS OF A.F. CORRELATION IN CUPRATES

1. Overall width of the peak of $\mathrm{Im}\,\chi(q,\omega)$ around $q \sim Q$
   $\rightarrow$ T insensitive
2. "Fermi surface effect" ("k_F-effect") or $\mathrm{Im}\,\chi(q \sim Q, \omega)$ (fine structure) $\rightarrow$ T dependent
3. $\left\{\begin{array}{ll} \frac{1}{T_1} \sim \text{const.} & \text{at high temp.} \\ \frac{1}{T_1} \sim T & \text{at low temp.} \end{array}\right.$ CROSSOVER
4. $\int S(Q,\omega)\,d\omega \sim \delta^{-1}$
   Q : coarse grained
5. q-integrated intensity around $q \sim Q$
   $\int dq\, \mathrm{Im}\,\chi(q,\omega) \rightarrow \begin{cases} \text{single parameter scaling by } \omega/T \\ \text{no} \end{cases}$
6. $\begin{cases} (T_1 T)^{-1} \sim (T_{2G})^{-1} \\ (T_1 T)^{-1} \sim (T_{2G})^{-2} \end{cases}$

1. $\int S(q=0,\omega)\,d\omega \propto \delta^{-1}$ $\leftrightarrow$ Endoh et al.

2. $T_1^{-1} \propto \begin{cases} T & T < T_{scr2} \\ \text{const} & T > T_{scr2} \end{cases}$ $\leftrightarrow$ Imai et al.

3. temperature independent ξ at $T < T_{scr1}$

4. $Q \equiv \lim_{\omega \to 0} \mathrm{Im}\,\chi(q,\omega)/\omega$

$$Q \propto \begin{cases} \text{const} & T < T_{scr2} \\ T^{-1} & T > T_{scr2} \end{cases}$$

5. $\int \mathrm{Im}\,\chi\, dq$

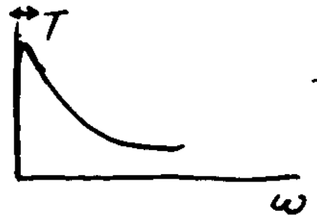

$T > T_{scr2}$

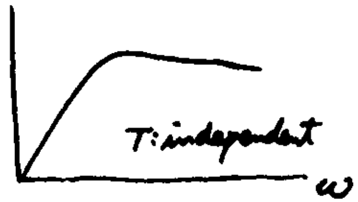

$T < T_{scr2}$

6. universal scaling of $\int \mathrm{Im}\,\chi(T)\,dq / \int \mathrm{Im}\,\chi(T=0)\,dq$ by a single parameter ω/T

※

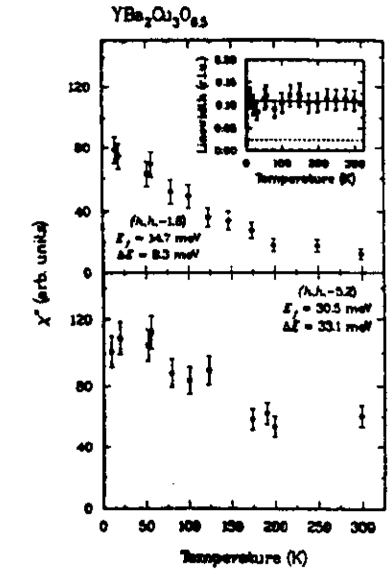

FIG. 4. Temperature dependence of $\chi''(\omega)$ at 8.3 and 33.1 meV. Points represent the peak intensity of constant-E scans determined after fitting to a Gaussian line shape and correcting for background. Data have been corrected by the Bose factor. The temperature dependence of the linewidth (full width at half maximum), measured in reciprocal lattice units (r.l.u.), is shown in the inset.

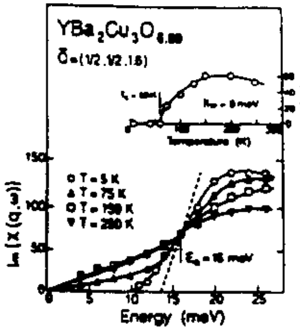

FIGURE 7

Im (χ(q,hω)) (in arbitrary unit) as a function of the energy for $YBa_2Cu_3O_{6.60}$ below (T = 5 K) and above (T = 75, 150, 250 K) the superconducting transition (T_c = 39 K). An energy gap ($E_G \approx 16$ meV) in the spin excitation spectrum clearly persists above T_c.

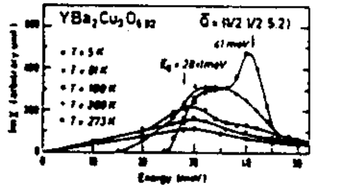

FIGURE 11

Im (χ(q, hω)) (in arbitrary unit) as a function of the energy for $YBa_2Cu_3O_{6.92}$ for increasing temperatures below and above T_c = 91 K. An energy gap (E_G = 28 meV) is clearly seen in the spin-excitation spectrum.

Neutron Scattering Data

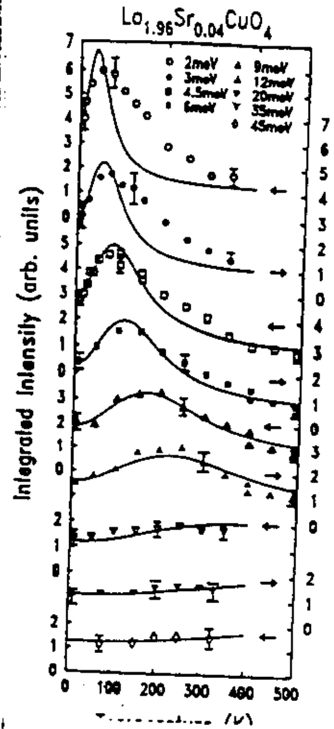

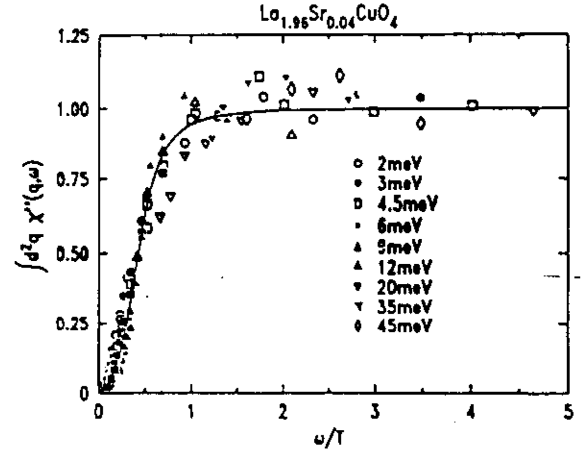

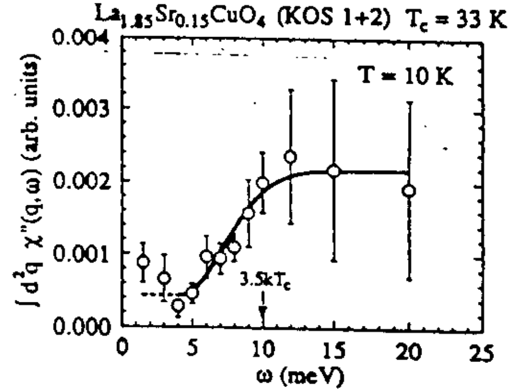

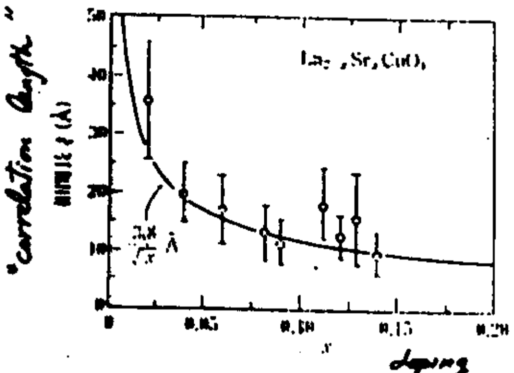

第 5 図　$La_{2-x}Sr_xCuO_4$ の 二次元スピン相関長のキャリアー濃度変化.

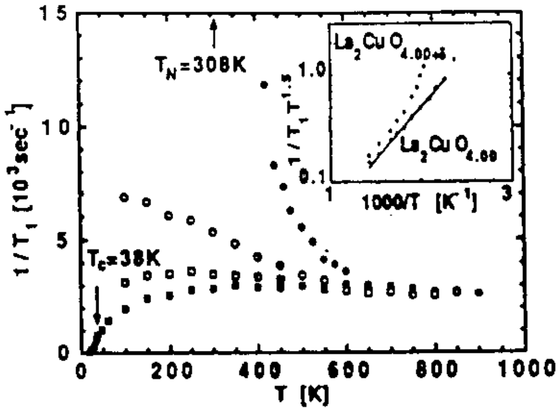

FIG. 2. Temperature dependence of $^{63}1/T_1$ measured by NQR for $La_{2-x}Sr_xCuO_4$ (●, $x=0$; ○, $x=0.04$; □, $x=0.075$; ■, $x=0.15$). The data below 100 K for $x=0.15$ are from Yoshimura *et al.* in Ref. [5]. Inset: The semilogarithmic plot of $^{63}1/T_1T^{3/2}$ (in units of $sec^{-1}K^{-1.5}$) vs $1000/T$ for the clean sample of $La_2CuO_{4.00}$ and for $La_2CuO_{4.00+\delta}$. The solid curve is the best fit by Eq. (2).

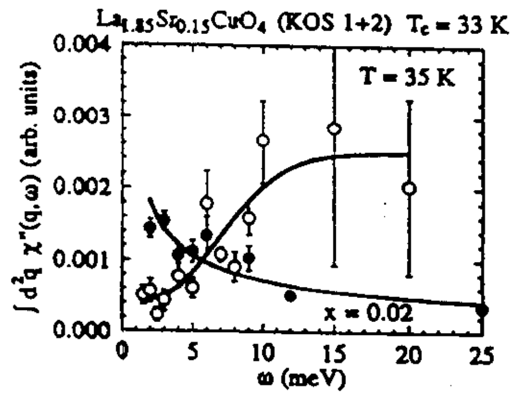

CONCLUSION

- Most of A.F. correlations are accounted [illegible] by the present theory in δ, T, and [illegible] plane [illegible] of "spin gaps" [illegible] seemingly controversial data. [illegible] neutron scattering are [illegible] consistent [illegible].

[illegible]

- [illegible] predictions for further experiments [illegible]

[illegible]

$Re\,\chi(q,\omega)$
$Im\,\chi(q,\omega)$
$S(q,\omega)$

- [illegible] theory with [illegible] quantitative analyses

Hints for MI transition in cuprates

1. 2D Hubbard QMC data

$$\chi_c \propto \delta^{-1}$$

$$\frac{m_c^*}{m_c} \to \infty$$

$$\Updownarrow$$

2. Experiments in cuprates
   - specific heat γ
   - Hall coefficient R_H

3. Comprehensive theory of Mott transitions

Two types of Mott transitions $\left\langle \begin{array}{l} m_c^* \to \infty \\ n_c \to 0 \end{array} \right.$

single-component vs. multi-component

$$\Downarrow$$

CROSSOVER BETWEEN SINGLE-COMPONENT AND MULTI-COMPONENT

DUALITY OF MOTT TRANSITION IN CUPRATES

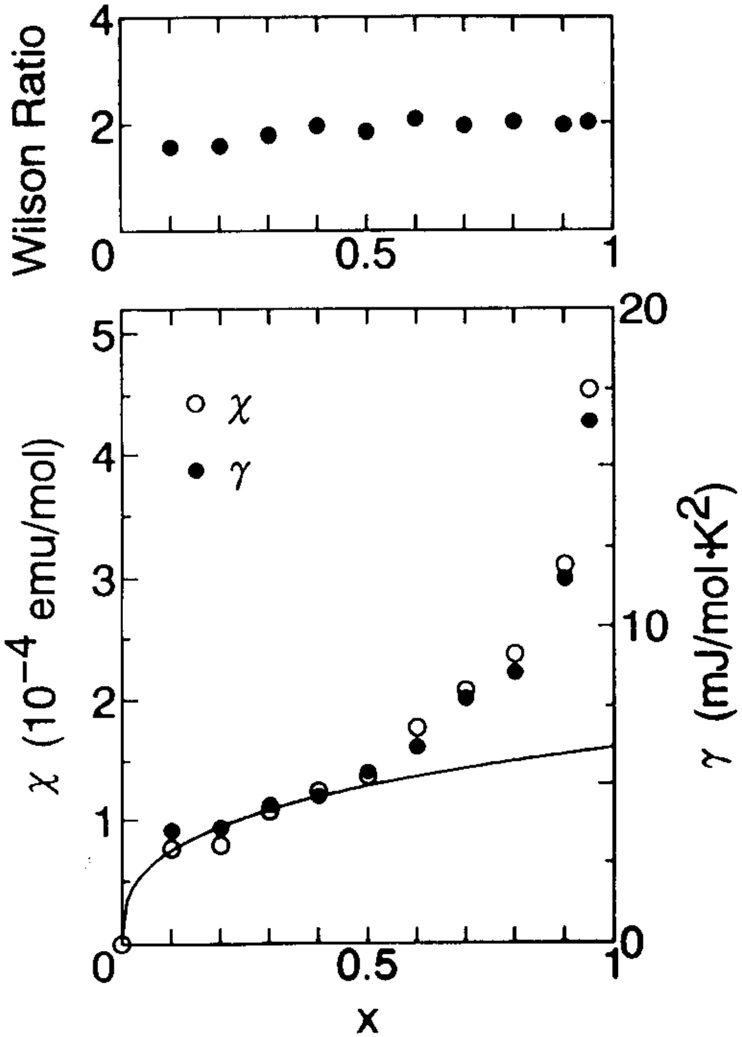

$La_x Sr_{1-x} Ti O_3$

Tokura et al.

Fig.3 Tokura et al.

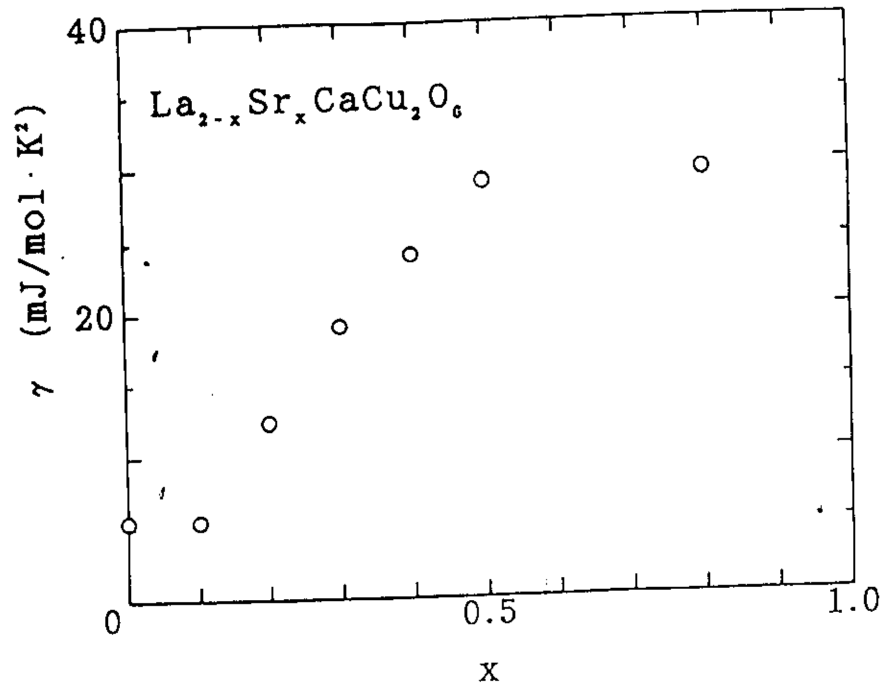

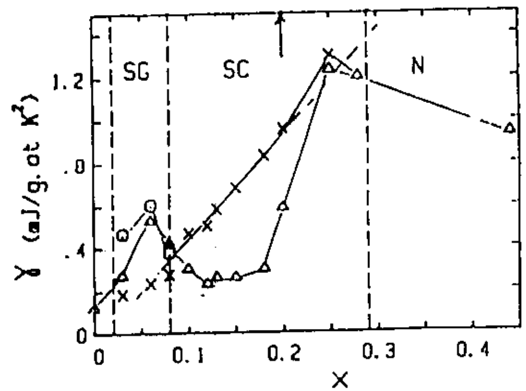

J.W. Loram et al.
Physica C 162-164 (1989) 498-499

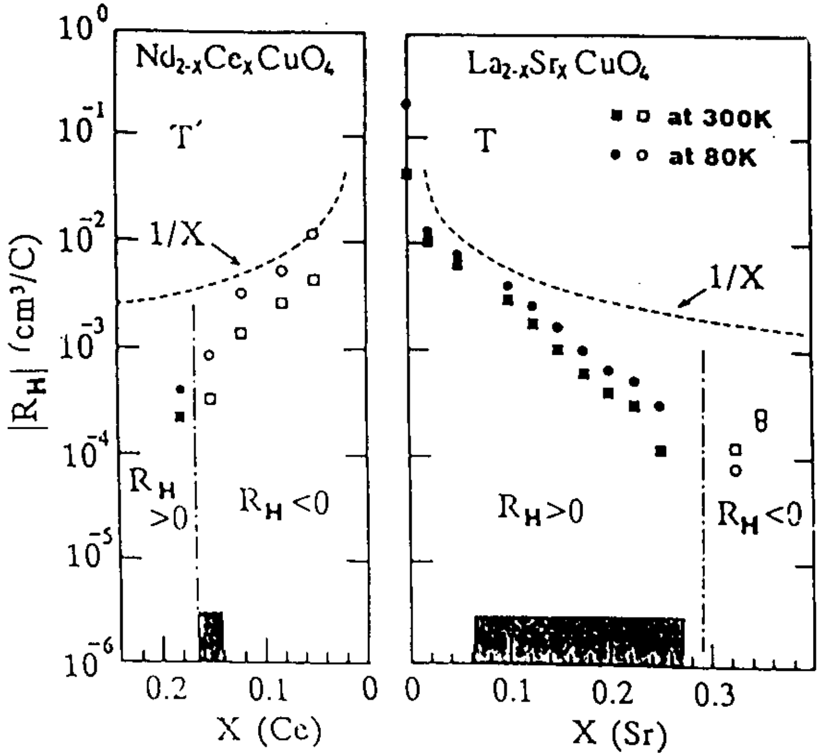

Fig. 8 The absolute value of the Hall coefficient as a function of Ce composition for reduced $Nd_{2-x}Ce_xCuO_{4-y}$. The same ploted for $La_{2-x}Sr_xCuO_4$ are show for composition. The shaded are a indicates composition region where superconductivity is observed.

S. Uchida et al.

Nishikawa, Takeda, Sato

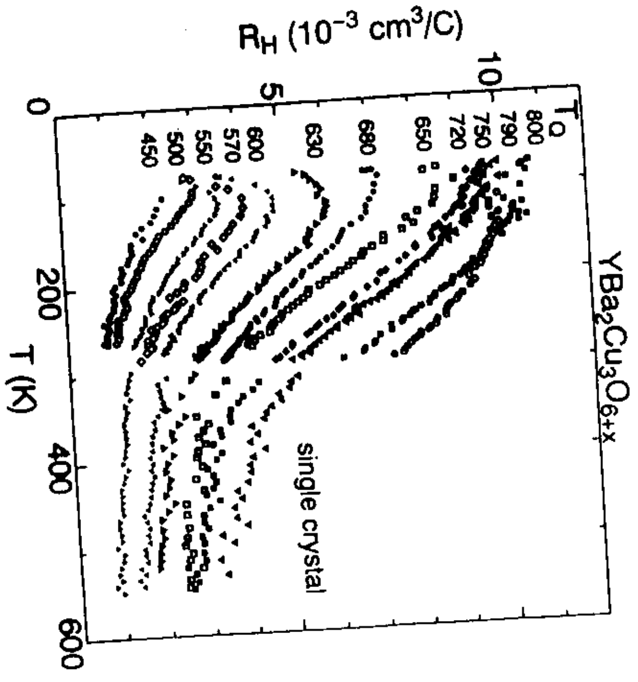

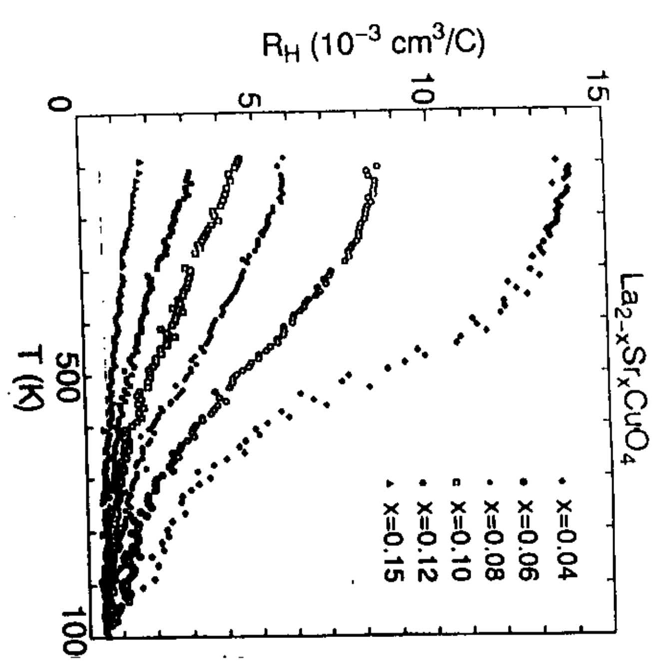

Duality in cuprates

— ONE SCENARIO —

LOW TEMP. | HIGH TEMP

$n \to 0$ $\xleftrightarrow[\sim 500\,K]{\text{CROSSOVER}}$ $m^* \to \infty$

in gap" | 2D Hubbard

single-component $\longleftrightarrow$ bi-componen

Hall coeff.
plasma freq.
specific heat

charge compressibility

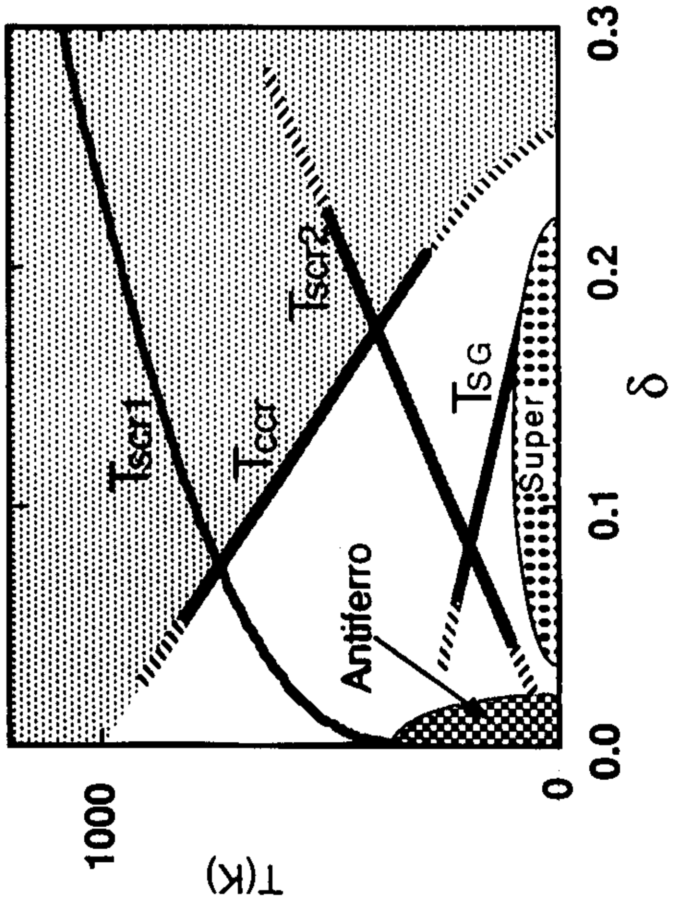

summary
New Field of Quantum Phase Transitions

- Metal-Insulator (Mott) Transition
- Antiferromagnetic Transition

CRITICALITY $\longleftrightarrow$ CROSSOVER

metal $\leftrightarrow$ insulator

ssification of ... Transition

$m_c^* \to \infty$ multi-component $z=4$

$n_c \to 0$ single-component $z=2$

1D, 2D spin-charge separation

metal $\leftrightarrow$ metal

single-component $\leftrightarrow$ multi-component

$\rightarrow$ cuprates
duality

AF $\leftrightarrow$ para.

difference from $T \neq 0$ critical phenomena
unified picture of spin correlation in cuprates
phase diagram of cuprates in (δ, T) plane

40